

Results from the Relativistic Heavy Ion Collider

Berndt Müller

Department of Physics, Duke University, Durham, NC 27708-0305

James L. Nagle

Department of Physics, University of Colorado, Boulder, CO 80309-0390

KEYWORDS: Quantum Chromodynamics, QCD, Relativistic Heavy Ion Collisions, RHIC, quark matter, quark-gluon plasma, QGP, deconfinement, chiral symmetry restoration

ABSTRACT: We describe the current status of the heavy ion research program at the Relativistic Heavy Ion Collider (RHIC). The new suite of experiments and the collider energies have opened up new probes of the medium created in the collisions. Our review focuses on the experimental discoveries to date at RHIC and their interpretation in the light of our present theoretical understanding of the dynamics of relativistic heavy ion collisions and of the structure of strongly interacting matter at high energy density.

CONTENTS

The Science of RHIC	2
<i>Strongly interacting matter at high energy density</i>	2
<i>“The Quest for the QGP” revisited</i>	4
<i>Context in physics and astrophysics</i>	9
Overview of experimental results	10
<i>Global characteristics, yields, and spectra</i>	12
<i>Flow observables</i>	14
<i>Hard observables</i>	18
Interpretation of Results	21
<i>The “ideal fluid”</i>	21
<i>Energy loss jet tomography</i>	22
<i>Thermodynamic properties</i>	23
<i>Partonic collectivity</i>	25
Outlook	25
<i>Review of lower energy results</i>	25
<i>Future outlook for RHIC</i>	27
<i>Outlook for LHC program</i>	28
<i>Open theoretical problems</i>	29
Summary	32

1 The Science of RHIC

1.1 Strongly interacting matter at high energy density

The Relativistic Heavy Ion Collider (RHIC) at Brookhaven National Laboratory was constructed to investigate the properties of nuclear matter at ultra-high energy densities (1). The motivation for this research arose in the 1970s, first, from speculations about possible novel states of nuclear matter at supranuclear densities (2, 3), and soon afterwards, from the insight that the structure of matter should become simple at asymptotically high temperatures (4). The celebrated principle of *asymptotic freedom* states that the effective coupling constant α_s of quantum chromodynamics (QCD), falls with increasing momentum transfer q^2 or, equivalently, with decreasing distance between particles. In a thermal medium, the characteristic momentum transfer between (nearly) massless particles is of order the temperature T , and thus the effective coupling between quarks and gluons must become weak when T grows large. The complicated structure of nuclear matter at low temperatures, where it is composed of a multitude of hadronic particles, baryons and mesons, whose interactions are difficult to calculate with precision, is thus expected to give way at high temperatures to the relative simplicity of a plasma composed of weakly interacting quarks and gluons, the *quark-gluon plasma* (5, 6).¹

Numerical solutions of QCD, discussed below, tell us that the transition from a hadronic gas to a quark-gluon plasma should occur at a temperature of approximately 170 MeV. This value coincides with the “limiting” temperature of matter composed of hadrons first postulated by Hagedorn (7). The Hagedorn temperature, defined as the exponential slope of the mass spectrum of hadronic resonances, was later understood to be associated with the transition to a new phase of matter (9), where hadrons are dissolved into their constituents, quarks and gluons. The precise value of the transition temperature T_c , and how high the temperature must rise before the plasma can be considered as weakly coupled, can only be determined by accurate, nonperturbative simulations of the equations of QCD.

Over the past decade, such solutions have become available due to vastly improved numerical simulations of thermal QCD on a Euclidean space-time lattice. In this approach, one evaluates the path integral of the QCD partition function

$$Z_{\text{QCD}} = \int DA \prod_f D\psi_f D\bar{\psi}_f \exp\left(-\int_0^{1/T} d\tau \int d^3x \mathcal{L}_{\text{QCD}}[A, \psi_f, \bar{\psi}_f]\right) \quad (1)$$

by a sum over representative field configurations $A(x, \tau)$, $\psi_f(x, \tau)$, and $\bar{\psi}_f(x, \tau)$, where A denotes the gluon field, $\psi_f, \bar{\psi}_f$ the quark fields of various flavors f and their adjoints, and τ is the imaginary time. Thermodynamic variables are obtained as derivatives of $\ln Z$; thermal expectation values of other observables can be obtained by inserting the relevant expression for the operator into the path integral.

¹Note that this argument does not apply to cold (i.e. low temperature) nuclear matter at high baryon density, because the Pauli principle forbids most scattering processes among quarks, except those near the Fermi surface. As a result, the structure of asymptotically dense, cold quark matter is more complex. See (8) for a review.

The functional integral over the quark fields requires the evaluation of the determinant of a large space-time matrix, which is a numerically demanding task.² The numerical expense grows rapidly with decreasing mass of the quarks. Significant progress has been made on the evaluation of the integral (1) in recent years, mainly due to three innovations: Improvements in computer hardware permit much faster calculations (up to about 10^{10} floating-point operations per second); improved representations of the QCD action on a lattice have enhanced convergence to the continuum action; new lattice representations of the quark fields preserve the symmetries (chiral symmetry) of QCD in the massless quark limit. Calculations using the last improvement are presently under way.

These computational advances have allowed us to glean several insights into the properties of hadronic matter at high temperature and vanishing net baryon density. The value of the transition temperature T_c has been shown to lie in the range 160 – 190 MeV (10,11). For the physical values of the u , d and s quark masses, the nature of the transition has been found to be a continuous cross-over, characterized by narrow, but finite peaks in various susceptibilities (12). The effective number of thermodynamically active degrees of freedom, defined as the ratio between the calculated entropy density and entropy density of a massless Bose field (SB):

$$\nu(T) = \frac{s(T)}{s_{\text{SB}}(T)} \quad \text{with} \quad s_{\text{SB}}(T) = \frac{2\pi^2}{45}T^3, \quad (2)$$

rises very rapidly over a small temperature range around T_c and then levels off at about 80% of the value $\nu_0 = 16 + \frac{21}{2}N_f$ predicted for a thermal gas of non-interacting gluons and N_f flavors of massless quarks, as shown in Figure 1.

Many static properties of the high-temperature phase of QCD have been studied in detail by means of lattice simulations (13). Among these are the equation of state, i. e. energy density $\varepsilon(T)$ and pressure $P(T)$, quantities related to color confinement and spontaneous chiral symmetry breaking, such as the expectation value of the Polyakov loop $\langle L \rangle$ and the quark condensate $\langle \bar{\psi}\psi \rangle$, various susceptibilities, and the potential $V_{\bar{Q}Q}(r)$ between a pair of heavy quarks (14,15). The results of these studies confirm that a dramatic rearrangement of the internal structure of hadronic matter occurs near T_c , which is consistent with the notion that states with open color are liberated above T_c and chiral symmetry is restored, except for the small current masses of the light quarks, which is not of QCD origin.

Much less is known with certainty about the dynamical properties of this quark-gluon plasma, because the Euclidean lattice gauge theory does not permit a direct calculation of quantities related to real-time evolution. Some progress has been made toward the calculation of dynamical response functions by analytic continuation from imaginary to real time, but only in quenched QCD, i. e. in the absence of dynamical light quarks (16). Intriguing results of such calculations, indicating the survival of heavy-quark bound states up to temperatures of $2T_c$ or more, may well be artifacts of this uncontrolled approximation. Many dynamical properties of the high-temperature phase have been studied in the framework of the so-called hard thermal loop (HTL) effective theory (17). There are good

²In the so-called *quenched approximation* this determinant is replaced by a constant. This procedure amounts to the neglect of all thermal quark-antiquark excitations, which is generally not a good approximation at finite temperature. Results obtained with this approximation must be considered with caution.

arguments in support of the notion that these techniques work reliably for temperatures $T > 3T_c$ (18,19), but it is not known precisely how low in temperature they can be applied and to which extent they work in the range of temperatures $T_c < T < 2T_c$ accessible in experiments at RHIC.

There have been speculations that the matter, which can be produced and studied at RHIC, is very different from a plasma of weakly interacting quarks and gluons (20). For common electromagnetic plasmas the well established measure of the interaction strength is the ratio between the average potential energy between neighboring ions and their kinetic energy: $\Gamma = E_{\text{pot}}/E_{\text{kin}}$. Plasmas with $\Gamma \ll 1$ are called weakly coupled, those with $\Gamma \gg 1$, strongly coupled (21). Unfortunately, this criterion is not applicable to matter composed of (nearly) massless, relativistic particles, such as the quark-gluon plasma, because the potential energy is not a well defined concept for such a system. A well defined measure of the interaction strength in a quark-gluon plasma is the ratio between its shear viscosity η (crudely speaking a measure of the mean free path of particles) and its entropy density (a measure of the inter-particle distance) (22). In the weak coupling limit this ratio behaves like (24, 25)

$$\eta/s \sim (\alpha_s^2 \ln 1/\alpha_s)^{-1}. \quad (3)$$

A small η/s ratio thus implies strong coupling. Since quantum mechanics limits the size of cross sections via unitarity, the ratio cannot be arbitrarily small. It has been conjectured that $\eta/s = 1/4\pi$ represents an absolute lower bound (22), and it has been shown that this value is reached in the strong coupling limit of certain super-symmetric gauge theories (26). Because lattice QCD is presently unable to reliably calculate transport coefficients like the shear viscosity, we do not know what the value of η/s is for QCD near T_c .

As we shall discuss, experimental results from RHIC indicate that the matter produced in nuclear reactions has a small ratio η/s . This finding has reinforced speculations that the quark-gluon plasma near T_c a strongly coupled one with the properties of a liquid with very low viscosity rather than a dilute gas (23). Whether this is connected with an internal structure that is dominated by quark-gluon bound states, as has been hypothesized (20), remains unclear. Arguments have been given that, if a quasi-particle picture applies to the matter near T_c , these quasi-particles must carry the same quantum numbers as quarks (27,28). These arguments do not rule out a more complex structure of the gluonic component of the matter.

It is appropriate to ask whether the quark-gluon plasma near T_c displays other liquid-like properties besides a small viscosity. One property that often differentiates liquid forms of matter from gaseous ones is that liquids are generally rather incompressible, at least when compared with gases. Unfortunately, it is not clear how to apply this criterion to the quark-gluon plasma, since at net baryon number zero ($\mu_B = 0$) and fixed temperature the pressure P is independent of the volume V . Whether other aspects of liquid-like behavior apply to the quark-gluon plasma near T_c is an open question.

1.2 “The Quest for the QGP” revisited

The experimental observation and study of the quark-gluon plasma must be based on signals which can provide evidence of its formation and permit a characterization of its properties. Our evolving theoretical insight into the nature of this new

state has also led to refinements in our understanding of these signals. Even if the transition between matter composed of hadrons and the quark-gluon plasma state is only a rapid, but continuous cross-over, we can still make a clear observation of the new state if we understand some of the key properties that define it.

The experimental quest must proceed in steps: First, the determination that the particles produced in the nuclear reaction really form, for a brief period, matter that deserves a description in thermodynamic terms; second, the determination that this matter has a novel structure and is not just a dense gas of hadrons; and third, the characterization of its main physical properties. In practice, these three steps are intertwined. In this section, we first give an update on some of the signatures discussed in the review by Harris and Müller (1) and then focus on the new probes accessible at RHIC for the first time in heavy ion collisions, involving hard QCD scattering processes.

1.2.1 Update on QGP signatures

We start with an update of quark-gluon plasma thermodynamics and probes of physics at the thermal energy scale.

- *Degrees of Freedom:* The lattice calculations predict that the effective number of (massless) degrees of freedom ν , as defined in Equation (2), assumes a value around 30 nearly independent of temperature above $1.2T_c$. This behavior is very different from that of a hadronic gas, for which the effective number of degrees of freedom will steadily increase with temperature as more and more resonances are excited. It is important to note that the thermodynamic definition, Equation (2), of the number of degrees of freedom does not necessarily imply that these are associated with well-defined, particle-like excitations, usually called quasiparticles. For temperatures near T_c , the quark-gluon plasma is quite likely strongly coupled, and we presently do not know what its dynamical excitations are. In fact, we do not know whether it contains any well defined quasi-particles which account for the value of ν deduced from the lattice simulations. This is important, because it warns us that an experimental determination of ν does not, in and of itself, tell us that the elementary carriers of color, quarks and gluons, are deconfined in the sense that they can propagate freely over distances larger than the size of a hadron (1 fm/c) without undergoing violent interactions.
- *Equation of State:* The lattice simulations of QCD tell us that the speed of sound c_s , defined by $c_s^2 = \partial P / \partial \varepsilon$, drops strongly below the value $c_s = c / \sqrt{3}$ valid for an ideal gas of massless particles, as T approaches T_c from above (c denotes the speed of light) (29). c_s is expected to reach a minimum near T_c and then increase again in the hadronic gas domain. This has potentially observable consequences for the transverse expansion of the fireball. The minimum of the function P/ε is called the “softest point” of the equation of state. If the matter is produced with initial conditions near this point, the driving force of its expansion is minimal, leading to an increase in the lifetime of the fireball (30,31).
- *Fluctuations:* Statistical fluctuations of conserved quantum numbers in localized phase-space domains can be related to the corresponding susceptibilities of the matter. Susceptibilities measure the effect of a change in

a certain intensive thermodynamic quantity, such as the temperature or a chemical potential on the associated extensive quantity, such as entropy or a conserved quantum number. They thus tell us how the system reacts to a change of external conditions. A second-order phase transition is characterized by certain divergent susceptibilities, such as the specific heat. Lattice simulations can make model independent predictions for such static quantities. From the experimental point of view, the most interesting quantities are the susceptibilities associated with the electric charge Q , strangeness S , and baryon number B (32, 33). The lattice calculations predict that the associated susceptibilities change strongly across T_c . In particular, the flavor off-diagonal susceptibilities rapidly vanish above T_c (34, 35), indicating that the thermodynamically relevant degrees of freedom carrying flavor and electric charge have the precise quantum numbers of quarks and antiquarks, but not of quark-antiquark pairs as in a hadron gas (27).

- *Chiral Symmetry Restoration:* The approximate chiral symmetry of QCD is spontaneously broken by the existence of a quark condensate in the vacuum. Lattice simulations predict a very rapid drop of the scalar quark condensate $\langle \bar{q}q \rangle$ from its vacuum value to almost zero in a narrow temperature region around T_c . The experimental observation of the predicted partial restoration of chiral symmetry above T_c is more difficult, because quarks are predicted to retain sizable self-energies at high temperature (36, 37). Although these do not break chiral symmetry, they are not easily distinguished from true scalar masses.

One way of identifying the onset of chiral symmetry restoration would be an observation of the gradual disappearance of the mass splitting between hadronic states of opposite parity, but otherwise equal quantum numbers. The most promising way of achieving this is to measure the in-medium mass shifts of vector mesons and their chiral partners, such as the ρ and a_1 mesons (38). This goal is complicated by the fact that the decays of the a_1 meson involve hadrons in the final state and thus are difficult to observe when they occur inside a dense medium.

Finally, a temporary restoration of chiral symmetry could manifest itself in the formation of local disorientated domains of the chiral order parameter matrix $\langle \bar{q}_\alpha q_\beta \rangle$ (α and β denote quark flavors). Such domains of disorientated chiral condensate (DCC) could be formed when the symmetry breaking is restored as the fireball cools rapidly through a second-order phase transition (39) (for a review, see (40)). A related, but even more speculative phenomenon would be the formation of parity- or CP-violating metastable vacua of the pion field (41).

- *Screening of Color Charges:* Perturbation theory predicts that the forces between color charges are screened at high temperature. Recent lattice simulations have confirmed this prediction, but also generated some uncertainty with respect to the phenomenological consequences of color screening. Lattice determinations of the potential between a heavy quark pair in a color singlet state (14), combined with a potential model of heavy quarkonia, suggest that the charmonium ground state J/ψ should cease to exist above $T_\psi \approx 1.1 T_c$ and the ground state of the $(b\bar{b})$ system above $T_\Upsilon \approx 2.3 T_c$ (42). On the other hand, direct analysis of the spectral function of the $(c\bar{c})$ system in quenched QCD by means of the analytic continuation of imagi-

nary time correlators indicates the survival of a narrow J/ψ state up to at least $1.5 T_c$ (43,44). It is presently unclear whether this result is an artifact of the quenched approximation or the analytic continuation procedure, or whether it indicates a failure of the potential model for charmonium at finite temperature (45).

Even if charmonium states survive significantly above T_c as bound states or narrow resonances, their production in heavy ion collisions may be strongly suppressed by reactions in the hot medium. The $(c\bar{c})$ pair, which can be produced in either the color singlet or color octet state, originally forms a highly localized state which then expands to hadronic size on a time scale dictated by the radius of the bound state (about 0.3 fm/c for J/ψ). In the presence of a thermal medium the formation of the bound state may be jeopardized if the relative momentum of the pair is increased by elastic collisions with constituents of the medium during this formation time (46). Even after formation of the bound state, the pair can be dissociated by inelastic collisions, which excite the internal wave function above the open charm threshold (47).

- *Thermalization:* An important component of the phenomenology of probes of the hot medium created in nuclear collisions at RHIC is the theory of initial formation of a high energy density state, its equilibration, and its evolution. Much progress on understanding these problems has been made over the past decade. A semiclassical description of the initial-state gluon fields in the colliding nuclei has allowed theorists to make detailed predictions for the space-time and momentum space distribution of partons in the pre-equilibrium phase of the reaction (48–50). It is now believed that perturbative QCD processes do not lead to a very rapid equilibration and thermalization of the initial parton distribution (51–53) (but see (54, 55) for contrasting opinions). An alternative pathway to thermalization, which has recently been studied extensively is furnished by instabilities among the soft gluon modes in a partonic medium with an anisotropic momentum distribution (56–60). It is not yet clear whether this mechanism reduces the thermalization time significantly compared to the perturbative thermalization scenario or just causes the parton distribution to rapidly become isotropic (61, 62).
- *Dynamical Properties:* Lattice simulations are presently unable to make reliable predictions of most dynamical properties of the quark-gluon plasma. Recent attempts to determine the real-time spectral functions for excitations of various color-singlet channels (16, 63, 64) are limited by the need to use the quenched approximation, and the results show inconsistencies, especially for low frequencies (65). The calculation of phenomenologically relevant transport properties, such as the shear viscosity or collective modes, remains an important challenge (66).

However, recently there has been important progress in calculating these dynamical properties perturbatively in a dual quantum field theory involving black holes in anti-de Sitter (AdS) space (22). This approach is based on the insight derived from string theory that weakly coupled gravity theories in higher dimensions can be dual to four-dimensional gauge theories in the strong coupling limit (67). It must be emphasized that these AdS/CFT (conformal field theory) techniques presently have the limitation that no

higher dimensional gravity or string theory is known which is dual to QCD. However, recent progress in calculating hadron structure and scattering processes make this an area to watch in the future (68).

1.2.2 New probes of the medium

One of the greatest recent advances in heavy ion physics is that, at the RHIC energies, one finally has access to hard processes where perturbative QCD (pQCD) calculations provide a solid theoretical framework (69). Ideally we would like to probe the created medium at different times as the system is expanding and becoming more dilute. One limitation is that all probes of the medium must be generated in the collision itself, and we must quantitatively understand their initial production cross sections in order to consider them as controlled and calibrated probes. The following list covers a few of the hard probes of dense matter relevant to the experiments at RHIC.

- *Factorization of QCD cross sections:* Parton-parton reactions involving large momentum transfer can result in back-to-back jets which have been well described at hadron colliders in terms of pQCD parton-parton cross sections augmented by experimentally determined initial parton distribution functions (PDF) and final fragmentation functions (FF). This framework assumes that the hard scale of the parton-parton interaction can be separated (“factorized”) from the soft, non-perturbative physics governing the PDF and FF. It further assumes that these functions are universal, i.e. they can be determined from well understood processes, like deep-inelastic scattering or $e^+e^- \rightarrow$ jets. If this factorization and universality can be shown to apply at the modest p_T range accessible at RHIC ($p_T^2 \approx 10 - 1000 \text{ GeV}^2/c^2$), then perturbative quarks and gluons constitute a calibrated probe which can be used to determine properties of the medium, for example, the color opacity (70). We will show in Section 2.3 that the RHIC data, indeed, support this notion.
- *Nuclear modifications of parton distributions:* One caveat is that it is well established that PDF are modified in nuclei relative to the proton by processes called shadowing, EMC effect, etc. For recent reviews see (71, 72). Partons carrying a very small momentum fraction x of the parent nucleon are generally depleted in nuclei compared with the proton. One model for understanding this depletion of low- x partons in nuclei asserts that the rapid growth of gluons must saturate when the density reaches occupation numbers of order α_s^{-1} (73). In this saturation scenario the nucleus is more appropriately described as a single gluonic wave function, sometimes referred to as the Color Glass Condensate (CGC) (74). Because the scale Q_s at which gluon saturation occurs grows with nuclear mass (75), it has been proposed that this process may be described perturbatively for large nuclei, especially at very high energies (76). A key test of the importance of nuclear modifications of parton distributions already at RHIC energies was to check if one could observe significant suppression effects on jets as an initial state effect from the nuclear (^{197}Au) wave function (77).
- *Parton energy loss:* Once an energetic parton is injected into the medium via a hard scattering event, it can lose energy and momentum by rescattering within the medium. We can distinguish three types of interactions of the

parton with the medium: If the parton elastically scatters on a structureless color charge, this will not result in an appreciable energy loss but in a random walk of transverse kicks. In order to scatter inelastically, a parton can either transfer some of its energy to a bound constituent of the medium or lose energy by radiating a gluon. In all three cases, the interaction strength (and in the latter two, the energy loss) is proportional to the density of color charge carriers in the medium and square of the color charge of the parton. Thus, a gluon, whose color charge is $3/\sqrt{2}$ times as large as the color charge of a quark or antiquark, should lose approximately twice as much energy as a quark in the same medium.

For light quarks and gluons with a large momentum, the dominant mechanism of energy loss is expected to be gluon radiation. The radiative energy loss ΔE of a massless parton penetrating a strongly interacting medium can be expressed in terms of a transport coefficient \hat{q} characterizing the stopping power of the medium and defined as (78, 79)

$$\hat{q} = \rho \int dq^2 q^2 \frac{d\sigma}{dq^2} = \langle q^2 \rangle / \lambda_f, \quad (4)$$

where ρ denotes the density of scattering centers, σ is the elastic scattering cross section, and \vec{q} the momentum transfer in a collision of the parton with a medium constituent. λ_f is the mean free path of the parton in the medium. In a static, homogeneous medium, the average energy loss depends quadratically on the penetration length L . The unusual dependence results from the rescattering of the radiated gluon in the medium in combination with the coherence of the radiation from scatterings occurring in rapid succession (called the Landau-Pomeranchuk-Migdal effect (80, 81)).

For a comparison with the RHIC data, one needs to take into account that the medium created in a nuclear collision at RHIC is not static and homogeneous. This can be done by defining an effective path length (83). In addition, it is important to use the full energy loss distribution $P(\Delta E)$ instead of the average energy loss $\overline{\Delta E}$ (82). It is also important to recognize that the requirement of emission of an energetic hadron increases the weighting toward large values of the fragmentation variable z and favors the near-surface emission of the hard parton (84, 85).

- Because their creation represents a hard QCD process, which can be calculated within the framework of pQCD, heavy quarks can also serve as hard probes of the hot medium (87). Besides their role as probes of color screening, heavy quarks also probe the color charge density in the medium through their energy loss, when they are created with a sizable transverse momentum. Their interaction with the medium differs from that of light quarks and gluons, because at leading order in the QCD coupling constant heavy quarks only interact with gluons in the medium. In addition, gluon radiation from a heavy quark with mass M and energy E is strongly suppressed at forward angles $\theta < \theta_0 = M/E$ (88). This “dead cone effect” (89) reduces the radiative energy loss of heavy quarks for moderate p_T .

1.3 Context in physics and astrophysics

One motivation for the construction of RHIC was the desire to explore the physics of matter under conditions that existed during the first 10–20 μs of our universe

in controlled experiments.³ If the deconfinement transition were a strong first order phase transition, it would have proceeded via bubble nucleation (91). The formation of macroscopic bubbles would have led to violent processes that would have left traces observable today (for a recent review see (92)). The two most important processes associated with bubble formation are the creation of local inhomogeneities in the cosmic baryon density during the time of nucleosynthesis and the possible formation of (meta-)stable strange quark matter nuggets (93). Both of these possibilities appear to be ruled out by the absence of a strong first-order phase transition in the equation of state predicted by lattice gauge theory.

One observable effect of the cosmological QCD phase transition, in principle, is the modulation of the spectral density of primordial gravitational waves due to the modification of the Hubble expansion as a result of the change in the number of light degrees of freedom (94). The modulation caused by the QCD transition is almost independent of the type of transition. If strongly first order, the transition itself could also have generated gravitational waves due to collisions among large nucleating bubbles (93). The interesting frequency range of gravitational waves is near 100 nHz. Unfortunately, no technique capable of observing gravitational waves in this frequency range is known today. Thus, the study of heavy ion collisions may provide the best insight on this early epoch in our universe, rather than the observation of the cosmological transition itself.

The unanticipated liquid-like nature of the quark-gluon plasma created in collisions at RHIC suggests analogies to the physics of strongly coupled electromagnetic plasmas (95). For such plasmas, the viscosity is large both in the limits of weak and strong coupling and attains a minimum at intermediate coupling. Interestingly, the naive application of classical measures of the coupling strength to the quark-gluon plasma near T_c also gives values in this intermediate range of values of the interaction measure (96).

Phenomena analogous to the anisotropic collective expansion of the matter produced in heavy ion collisions have recently been observed in degenerate systems of fermionic atoms released from optical traps (97). These systems exhibit many features associated with superfluidity, and their collective flow is probably governed by collisionless ideal fluid dynamics. It is an intriguing question whether the physics underlying the nearly inviscid transverse flow of matter produced in relativistic heavy ion collisions is of a similar nature.

2 Overview of experimental results

2.0.1 Update on RHIC detectors

The Relativistic Heavy Ion Collider construction was completed in 1999 with the first physics running the following year. The collider is located in a 3.8 km circumference tunnel and is composed of two identical, quasi-circular rings of superconducting magnets oriented to intersect at six experimental hall loca-

³In the inflationary Big Bang model, the universe first inflates in an ultracold (false vacuum) state and then reheats to a high temperature after making the transition into the true vacuum. Usually one assumes that the reheating temperature is far above the electroweak transition ($T \gg 100$ GeV). But the observational evidence only demands that the temperature generated by reheating after inflation exceeds about 4 MeV (90). It is thus not completely certain that the temperature range reached in the RHIC experiments was ever probed in the Big Bang.

tions (98). The machine can accelerate gold nuclei up to momenta of 100 GeV/c per nucleon in each beam and protons up to 250 GeV/c, and smaller mass nuclei up to intermediate momenta depending on their mass to charge ratio. The center-of-mass energy in these collisions is over an order of magnitude higher than the previous highest energy heavy ion reactions at the CERN SPS fixed target facility, and two orders of magnitude above the BNL AGS fixed target facility. The nominal design luminosity for gold nuclei at full energy of $2 \times 10^{26} \text{ cm}^{-2}\text{s}^{-1}$ was already achieved during the first two physics running periods.

There are four dedicated experiments for studying heavy ion physics at RHIC: BRAHMS, PHENIX, PHOBOS and STAR. Detailed descriptions of the detectors and their performance are given in (99). The experimental program was designed such the experiments contain not only unique capabilities, but significant overlap to provide essential cross checks.

The BRAHMS experiment has two movable, small acceptance spectrometer arms. A range of detector technologies allow them to identify hadrons (π, K, p) up to very large rapidity when the forward arm is positioned close to the beam line. The PHOBOS experiment utilizes silicon technology and covers nearly the full solid angle for charged particles, but with limited particle identification. Thus, the PHOBOS experiment has excellent global event characterization capability.

The PHENIX experiment is a combination of two detector systems. There are two spectrometers with limited rapidity coverage around midrapidity with excellent hadron, electron and photon identification capabilities. Additionally there are two muon spectrometers at forward and backward rapidity for measuring decays of heavy quarkonia states and single muons. A high speed trigger and data acquisition allow for nearly dead-timeless running. The STAR experiment is based around a large coverage Time Projection Chamber (TPC) inside a solenoidal magnet that provides exceptional charged particle tracking and particle identification via the measurement of ionization energy loss dE/dx . The large coverage allows for multi-particle correlation measurements and also reconstruction of multi-strange baryon decays. In addition, STAR has an electromagnetic calorimeter and additional forward angle detectors including a radial-drift TPC. The STAR data acquisition is high bandwidth and incorporates a multi-tiered trigger system. Schematic diagrams of the two large detectors are shown in Figure 2.

All experiments have been successful in being quickly commissioned and providing interesting physics results from the first running at RHIC. The accelerator has the flexibility to run multiple species and energy configurations each year. The different colliding species, energies and integrated luminosities to date are shown in Table 1.

During the early discovery phase, one focus of the experiments at RHIC has been establishing evidence for the formation of a thermodynamically equilibrated state of matter in gold-gold collisions. In addition, they have begun to address the following properties of the created medium:

- Its initial energy and entropy density;
- Its flavor composition and net baryon content;
- Its equation of state;
- Its shear viscosity;
- Possible collective modes;

- The quantum numbers of the carriers of collective flow;
- The characterization of jet quenching;
- Heavy quarkonia suppression;

The experiments have published an extensive set of refereed publications to date. In addition, each experimental collaboration has published a review of all their results to date in a single volume (100–103).⁴

2.1 Global characteristics, yields, and spectra

When colliding two nuclei one wants to understand how the initial kinetic energy (39 TeV at RHIC in gold-gold reactions) is re-distributed after the collision in terms of particle production, energy per particle, collective motion, etc. An intimately related question is that of entropy production, since the initial nuclei form a very low entropy state and the final configuration has a very large entropy.

The BRAHMS experiment measures the rapidity distribution of protons and thus determines how much kinetic energy appears to be retained by the colliding nucleons (104). Their data indicate that in central gold-gold reactions, over 28 ± 3 TeV of energy is deposited in heating the newly created medium and collective motion. All four experiments measure the resulting distribution of this energy amongst newly created particles. The PHOBOS experiment with measurements over nearly the full solid angle observes the creation of approximately 5000 charged particles and thus 7500 total particles, based on estimates of the neutral particle contribution (105). The production of nearly 20 particles per incident nucleon implies a large entropy production. A critical task is determining when and how this entropy is produced.

The experiments have also measured the charged particle multiplicity as a function of collision energy and centrality (impact parameter). The growth of multiplicity with increasing collision energy (100–103) is less than expectations from in a simple picture of “soft” coherent production combined with “hard” mini-jet production that increases quickly with increasing energy (106). An alternative description of the multiplicity dependence was proposed in the context of saturation models where the incoming gluon density at low momentum fraction x in the incoming nuclei is suppressed. Color Glass Condensate (CGC) models which incorporate gluon saturation have had significant success in describing the data (107). Detailed tests of whether this picture captures the underlying physics are discussed later in the context of hard processes (see Section 2.3).

The PHOBOS experiment has made the observation that the charged particle multiplicity per participating nucleon pair in central gold-gold reactions is nearly identical to that measured in e^+e^- annihilation events at the same center-of-mass energy, again per participant pair for the heavy ion case (102). The agreement persists over the entire energy range at RHIC. Such scaling observations are striking and have yet to result in a detailed explanation in terms of, for example, global energy conservation. This agreement is particularly puzzling since the e^+e^- growth in multiplicity with energy is well described by perturbative QCD in terms of gluon splitting and then mapping partons into hadrons via parton-hadron duality (108).

⁴In general we will reference the original data publication, except in cases where the results are a compendium of results and we will refer to these so-called “White papers.”

Experiments have also measured the total transverse energy production in these reactions.⁵ One can relate the transverse energy to the energy density in the context of a boost-invariant cylinder scenario (109) which suggests an initial energy density of $15 \text{ GeV}/\text{fm}^3$ decreasing to $5.4 \text{ GeV}/\text{fm}^3$ by a time $t = 1 \text{ fm}/c$ as shown in Figure 3 (101). Although the energy density decreases as $1/\text{time}$ or faster, the energy density significantly exceeds the expected transition density from lattice QCD calculations for a time up to approximately $5 \text{ fm}/c$. It is notable that the CGC calculations when tuning the saturation scale Q_S to match the multiplicity, overpredict the transverse energy (or E_T per gluon which translates using parton-hadron duality into E_T per hadron). This may be reconciled if there is substantial longitudinal work done in the expansion which will decrease the total transverse energy. Dynamical models describing the three-dimensional evolution, which have recently become available (110), allow for the study of these effects in detail.

Almost the entire particle production can be described with a few simple parameters. One can calculate the yields of most hadrons ($\pi, K, p, \bar{p}, \Lambda, \Sigma, \Xi, \Omega, \phi$) near midrapidity in terms of a single temperature of order 170 MeV and a small light quark (baryon) chemical potential (μ_B), as shown in Figure 4 (100–103).⁶ One particularly striking feature is that even the multi-strange particles appear at chemically equilibrated levels.

The transverse momentum distributions of the emitted particles have also been measured, and in many cases the rapidity distributions as well (100–103). The mean transverse momentum $\langle p_T \rangle$ for pions is of order 400 MeV . If we translate this into three dimensions and multiply by the particle number (7500), we obtain only about 4 TeV . Thus, a very large fraction of the incident energy resides in the (collective) longitudinal motion of the medium. The PHOBOS and BRAHMS experiments in particular have characterized the longitudinal motion in rapidity space (102, 115). The identified pions follow a Gaussian distribution in rapidity with a width consistent with the prediction of the Landau hydrodynamical model (116). In this scenario, all of the incoming energy is rapidly thermalized in a volume the size of the Lorentz contracted overlapping nuclei which then expands hydrodynamically until the particles decouple. This model would imply all the entropy generation takes place in the very short overlap time of the two nuclei, $2R/(\gamma c) < 0.2 \text{ fm}/c$, followed by isentropic expansion. It would imply an enormous initial equilibrated energy density of about $3000 \text{ GeV}/\text{fm}^3$.

In the alternative Bjorken scenario (109) much of the initial incoming longitudinal momentum is transformed into longitudinal collective motion, and the system can be described as a boost-invariant cylinder of fireballs distributed in rapidity space. The Bjorken scenario is often invoked for simplicity, but the measured rapidity distributions do not show boost invariance. In addition, particle ratios and spectra are observed to vary significantly as a function of rapidity (117). The deduced baryon chemical potential is larger at forward and backward rapidities, as one might expect from the increased presence of remnants of the colliding nu-

⁵The transverse energy measurements to date are centered at mid-rapidity. Many of the experimental observations are in a window around mid-rapidity. We will make special note of important measurements at forward and backward rapidity.

⁶Hadron abundances containing charm quarks are not described by chemical equilibration as expected since their quark mass significantly exceeds the temperature. Additionally, unstable resonances such as the K^* deviate from chemical equilibration (114) potentially due to re-scattering of their daughter decay products.

clei in these regions of phase space. This observation shows that the system is intermediate between the limits of the Bjorken and Landau models.

The transverse momentum spectra of the particles are found to deviate from a static Fermi-Dirac or Bose-Einstein distribution (approximately Boltzmann for the temperatures and chemical potentials relevant for RHIC). However, the spectra are well described at low $p_T < 2$ GeV/c with a common Boltzmann component and a radial velocity boost from the outward blast of the medium (100–103). Simultaneous constraints from the transverse momentum spectra of many different hadron species (with a wide range of masses) and two-particle correlation results constrain these contributions. If one removes the common velocity boost component, one finds the measurements at midrapidity are consistent with black-body radiation from a hot medium. The particle ratios indicate that the emissivity of the fireball is nearly the same (most likely unity) for all stable hadrons.

It has been noted that the appearance of an exponential energy distribution of particles is not conclusive evidence for equilibration but can also be the result of phase space dominance of the final states. However, in elementary particle reactions, particles carrying non-zero strangeness are always suppressed (113), whereas in the nuclear reactions at RHIC their yields are in perfect agreement with the predictions of the thermal model. The simplest explanation of this observation is that the available energy is equilibrated over a large enough volume to approximate a grand canonical ensemble, including strangeness. In addition, there is significant evidence for intense re-scattering amongst constituents to favor a thermal intermediate state over a direct reaction with a final state dominated by phase-space.

One additional set of global observations relate to fluctuations. In any study of phase transitions, the measurement of particle number and energy fluctuations is very relevant. If the transition were strongly first order, one might expect the fireball evolution to involve large bubble formation from a supercooled phase, which could lead to large phase-space fluctuations within a single event and also significant event-by-event fluctuations. Predictions were also made that one could have domains (regions in phase space) with disorientated chirality (DCC, see Section 1.2) that would re-align their chirality through the emission of low p_T pions with anomalous isospin distributions (40). There have also been predictions of the formation of domains with strong CP violation (118).

These measurements are quite challenging and published results to date (101, 119) already indicate that multiple contributions to the fluctuations are likely. The non-statistical fluctuations may have contributions from jet fragmentation correlations, quantum statistical correlations, and for the case of hadrons with complementary quantum numbers (baryon-antibaryon or positive-negative charge pairs) conservation correlations (as described by balance functions (120)). No unambiguous statement on fluctuations from a particular phase transition can be made at present.

2.2 *Flow observables*

One of the most dramatic discoveries at RHIC is that the medium displays a high degree of collectivity, often referred to as flow. Since we compress nuclear matter in the early stages of the collision, if there are large interaction cross sections between constituents of the medium, we expect density gradients to translate into outward pressure that cause the system to explode at relativistic speeds.

In the previous section in discussing the p_T spectra of various hadrons, it was necessary to include an outward boost velocity $v_b/c > 0.5$ to describe the mass dependent differences.

Experiments can probe this outward pressure with great precision by characterizing non-central (intermediate impact parameter) nuclear collisions. In these reactions, the nuclear overlap region is not circular in the transverse plane, but instead elliptically shaped. Thus, the density distribution if decomposed into azimuthal angle Fourier components has many non-zero coefficients, with the second coefficient being by far the largest. The stronger the interactions amongst the particles, the greater the translation of spatial anisotropy into momentum anisotropy of the final observed particles. There are two key features of this flow behavior. First, the flow is self-limiting in that as the system expands the spatial distribution becomes more isotropic. Thus, a large contribution to the flow must come from interactions in the first 2 fm/c after the collision (121). Second, regardless of the constituents of the matter at these early times, the momentum anisotropy is preserved through any type of transition to the final observed hadron distributions.

Experimentally one measures the ϕ angular distribution of particles relative to the reaction plane angle Ψ_R for each nucleus-nucleus collision and then performs a Fourier decomposition. Experimentalists have developed sophisticated techniques for determining the reaction plane angle Ψ_R in each collision (101–103). The second component v_2 of the Fourier decomposition is found to be the largest and is referred to as elliptic flow.

$$\frac{dN}{p_T dp_T dy d\phi}(p_T, y, \phi; b) = \frac{dN}{p_T dp_T dy} [1 + 2v_2(p_T, y; b) \cos(2\phi) + \dots] \quad (5)$$

One can also determine these coefficients via two-particle correlations in ϕ and higher order particle correlations, referred to as the cumulant technique (122), which aids in eliminating “non-flow” contributions.

Experiments have extensively measured the v_2 coefficient for a broad range of hadron species, over a significant kinematic range (101–103). We emphasize that the experiments do not directly measure pressure gradients or flow, but rather the coefficients of the ϕ angle distributions. For example in proton-proton reactions one observes a significant v_2 coefficient due to hard parton-parton scattering creating opposing jets of hadrons. In heavy ion reactions the this Fourier decomposition really measures particle emission directly correlated with the orientation of density gradients as demonstrated by the fact that the v_2 for all charged particles at low p_T scales linearly with the eccentricity of the nuclear overlap region (i.e. the exact shape of the ellipse). Another striking confirmation comes from two-particle correlations resulting from Bose-Einstein quantum statistics. This effect is often referred to as Hanbury-Brown and Twiss (HBT) correlations (123) and a review of the methodology as applied to heavy ion reactions can be found in (124). The STAR experiment has measured the source emission size via HBT as a function of the orientation of the two particles relative to the reaction plane (125). These results confirm the spatial deformation consistent with expansion from the original ellipse shape.

In Figures 5 and 6 we show v_2 as a function of p_T for different identified hadron species. At low $p_T < 2$ GeV there is a striking splitting in the v_2 pattern where heavier particles have a smaller v_2 than lighter ones at a fixed p_T . This splitting has a natural explanation if the pressure causes the particles to be

boosted with a common velocity, as is the case in a fluid dynamical picture. Also, the increase of v_2 with p_T for all particles is expected as higher momentum particles have been given a larger velocity boost and are thus more strongly correlated with the maximum pressure direction. The exact pattern of splitting is sensitive to the equation of state of the fluid in this picture and may thus allow for an extraction of the equation of state to compare with lattice QCD results. An important additional measurement from the PHOBOS experiment indicates that v_2 drops significantly for charged particles as one moves away from midrapidity (126). This observation contradicts many hydrodynamic calculations invoking the Bjorken scenario (109). Additionally some have interpreted this as evidence for incomplete equilibration and thus a breakdown in the hydrodynamic assumption (127).

Measurements of two-particle (HBT) correlations provide significant additional constraints on the final space-time configuration calculated in fluid dynamical models. The experimental data (101, 103) reveal significant disagreements with these models when they match the v_2 and p_T spectra. This is often referred to as the “HBT puzzle.” Potential solutions to this puzzle are discussed in Section 3.1.

The spectra of even the heaviest hadrons, including the ϕ , Ξ , Ω , exhibit the same flow-like patterns as the lighter hadrons (128). In the case of the ϕ meson, its hadronic cross section with π , N is small due to OZI rules, which state that processes involving diagrams with disconnected quark lines are suppressed (129). One estimate of the inelastic cross section with nucleons yields $\sigma_{\phi N} \approx 9$ mb (130). The Ω also has a small inelastic cross section, in part due to the lack of π - Ω resonant excited states (133), but its value $v_2^{(\Omega)}$ is comparable to $v_2^{(N)}$. These small cross sections result in mean free paths for these hadrons that are large compared to the system size. Thus, in a hadronic scenario one might have expected the $v_2^{(\phi)}$ to be lower than $v_2^{(N)}$ despite their similar mass. Models that attempt to describe the physics in terms of scattering processes among quasi-free hadrons (such as RQMD, UrQMD, HSD) predict v_2 values for all hadrons at modest p_T about five times lower than those measured at RHIC (134). Some have argued that elastic scattering and $3 \rightarrow 2$ inelastic processes (135) not included in all hadronic models may significantly increase the expected flow. However, the hadronic densities required such that $3 \rightarrow 2$ processes dominate indicates that multiple hadrons occupy the identical physical space-time coordinates.

This indicates that the constituents of the matter during the early time period ($\tau < 2$ fm/c), during which the elliptic flow pattern is established, are not ground state hadrons interacting with their standard hadronic cross sections. A correlated consequence is that if the ϕ and Ω whose hadronic production cross sections are OZI suppressed are actually formed by the “coalescence” or recombination of $s\bar{s}$ and sss respectively, then we should expect their production to exactly match the chemical equilibration model, which the data confirm.

As shown in Figure 6 for $p_T > 2$ GeV, the pattern of v_2 for various hadrons appears to break down, and baryons have a v_2 larger than mesons – in contrast to the behavior at low p_T . Given the finite size and lifetime of the fireball, only a limited number of interactions between constituents can occur and thus a finite number of p_T kicks. This implies that above some p_T the continuous fluid approximation must break down. Naively, one might expect the v_2 values to saturate, as the data indicate, but the picture is complicated by the observation that the baryons and mesons saturate at significantly different values of v_2 . Again,

this may be a confirmation that these hadrons are formed from recombination of partons which themselves are the original carriers of the flow anisotropy.

A simple model can be formulated where the flow is carried by quark-like constituents (denoted as “ Q ”) with baryon number $1/3$. In this case, if the formation of hadrons results afterwards by coalescence of these “quarks”, baryons on average have three times the p_T of the constituents and $v_2(B) = 3v_2(Q)$. The same reasoning applied to mesons, with the presumption that a meson is formed by coalescence of a “ $Q\bar{Q}$ ” pair, predicts that mesons have on average twice the momentum of the constituents and $v_2(M) = 2v_2(Q)$. It is tempting to identify these medium constituents with the “constituent” quarks of the naive quark model. However, this is potentially misleading since we have no experimental information on their mass or composition. Nonetheless, for the model to work, the medium constituents must have the same quantum numbers as the valence quarks of the emitted mesons and baryons.

Another experimental piece of information adding to the so-called “baryon puzzle” comes from the relative yields of baryons and mesons in the intermediate momentum range $2 < p_T < 6$ GeV/c. The ratios of hadron yields, which are dominated by $p_T < 1$ GeV/c, are well described by the chemical equilibrium model. At the highest $p_T > 5 - 8$ GeV/c, the hadron yields appear to be consistent with jet fragmentation functions as determined from other hadronization processes. For example, in quark and gluon jets measured in proton-proton collisions the \bar{p}/π^- ratio is about 0.2 (136). However, at RHIC in central gold-gold reactions, the \bar{p}/π^- (137) and similarly $\bar{\Lambda}/K$ (138) ratios approach unity in the intermediate p_T range, as shown in Figure 7 (139). At the highest transverse momenta, even if partons propagating through the medium have large in-medium interactions (as detailed in Section 2.3), the leading parton is expected to punch out of the system before fragmenting in the vacuum. Thus, we may expect the ratio of hadrons above some p_T threshold to be universal. At more modest p_T , mass related formation time differences between baryons and mesons might result in significant deviations from the universal vacuum fragmentation ratios. However, the data do not support a picture which associates the peculiarities of the hadron ratios at intermediate p_T at RHIC with hadronic mass differences. For example, the ϕ -meson appears to follow a scaling from mid-central to central gold-gold collisions similar to the lighter mesons, rather than the equally massive nucleons (140). The simple model of recombination of quark-like constituents may also reconcile this part of the puzzle. Three of these constituents need to coalesce to form baryons and only two to form mesons. This mechanism effectively boosts baryons to larger p_T than mesons, and since the p_T spectra are rapidly falling, the yields of baryons are enhanced compared with meson yields at the same p_T .

These observations led the authors of (141) to reason that the “(recombination) scenario requires the assumption of a thermalized partonic phase characterized by an exponential momentum spectrum. Such a phase may be appropriately called a quark-gluon plasma.” However, other observations do not fit into such a simple picture. If the emission of the intermediate p_T hadrons would, indeed, occur by recombination from a well thermalized medium, these hadrons should not exhibit jet-like angular correlations. Experiments have made first measurements of such di-hadron correlations and found significant jet-like correlation for both, mesons and baryons (142). This finding lends support to speculations that hadrons in this p_T range are formed by a combination of “shower partons” from fragmenting jets and “thermal partons” from the medium. These models need to be further

tested with very high statistics data for identified particles.

In the first few years of RHIC running, it was assumed that c - and b -quarks were too massive to participate in collective flow. (Since most of their mass is of non-QCD origin, it is retained when chiral symmetry is approximately restored in the medium.) In a perfect hydrodynamical medium with zero mean free path, all particles must move with the same velocity field. However, the medium created in heavy ion reactions lasts only $10 - 20$ fm/c. Since the average thermal momentum of a heavy quark with mass $M \gg T$ is $\langle p^2 \rangle \approx 3MT$, it would require many interactions with momentum transfer of order T to thermalize a c - or b -quark and let it participate in the collective flow. However, recent data from the PHENIX experiment suggest that, contrary to the expectations, this may in fact occur (143) indicating even stronger interactions in medium.

One method of extracting heavy meson contributions is from the measurement of “non-photonic” electrons that are expected to originate mainly from semi-leptonic decays of D and B mesons (for example $D \rightarrow K + e + \nu$). Electrons at low p_T carry little kinematic information about the parent D meson, but for electrons with $p_T > 1$ GeV/c the azimuthal direction of the electron is well correlated with the angle of the parent D meson and the electron carries on average 60% of the p_T of the meson. The measurement is challenging since one must first measure the inclusive electron anisotropy and then subtract off the anisotropy resulting from “photonic” background (for example $\pi^0 \rightarrow \gamma e^+ e^-$).

The PHENIX experiment has measured the v_2 coefficient for these “non-photonic” electrons and deduced a significant anisotropy for D mesons (144). More precision data is needed to determine if these heavy quarks are flowing with the identical velocity field as the light partons.

2.3 Hard observables

As discussed in Section 1.2, the RHIC experiments have opened the door on using hard probes to study the medium created in heavy ion reactions. Before using these as probes, one must experimentally understand the initial hard scattering processes involved.

Measurements addressing the question whether modifications to hard scattering processes observed in nucleus-nucleus collisions are significantly influenced by initial-state effects were made using deuteron-gold reactions. In these reactions one could still have a depletion of jets or high p_T particles due to gluon saturation in the incoming gold nucleus, but since no substantial medium is created, there should be little chance for the outgoing partons to be modified as might occur in a nucleus-nucleus reaction. Results from all four experiments (145) conclusively show that hadrons at midrapidity with $p_T \approx 2 - 10$ GeV/c are not suppressed but rather show a modest enhancement, possibly due to initial and final state partonic multiple scattering (often referred to as the “Cronin effect” (146)). An important additional observation was made that at more forward rapidities, sensitive to even lower x partons in the gold nucleus, experiments observe a suppression of hadron production at modest $p_T \approx 2 - 5$ GeV/c (147). This effect is currently under intense investigation to see if it relates to gluon saturation or the CGC.

A second relevant observation is of direct photon production in gold-gold reactions. The direct photons are all photons emitted in the reaction excluding those from hadronic decays of π^0, η , etc. At low $p_T < 3$ GeV/c there may be significant direct photon contributions from thermal radiation by the medium

(see Section 4.3). At higher p_T we expect the direct photons to be dominantly from initial quark-gluon hard scattering processes. The PHENIX experiment has measured the yield of direct photons at midrapidity for $p_T = 2 - 14$ GeV/c in proton-proton reactions and finds the results in excellent agreement with NLO pQCD predictions (148). Because the final-state interactions of energetic photons are small, the yield of direct photons in gold-gold reactions can be described by multiplying the yield measured in proton-proton reactions with the ratio of the incident parton flux of two gold nuclei to that of two protons. This normalization is usually referred to as *binary collision scaling*. The data show the measured direct photon yield in gold-gold to be in perfect agreement with this expectation (148). Thus, even in these violent gold-gold reactions, factorization and universality seem to hold, with the emitted photon passing through the created medium unaffected. The fact that the parton flux of the incident gold nuclei is obtained by geometric superposition of the nucleon parton distribution functions (PDF) also demonstrates that nuclear modifications of the PDF are modest in this kinematic domain. We note that in the case of this measurement, we are not checking the fragmentation function (FF) factorization assumption since the photon is not strongly interacting.

After these tests of the calibration framework for hard scattering processes, we turn to the observations relevant to quark and gluon probes of the medium. In the first data taking at RHIC, the experiments observed jet quenching in the form of a suppression in the yield of high- p_T hadron production at midrapidity (100–103). Shown in Figure 8 is the nuclear suppression factor R_{AA} , which is the measured yield of hadrons relative to the expected yield from proton-proton reactions scaled according to the binary collision assumption, as a function of p_T for unidentified and identified hadrons. In contrast to the direct photon data, we observe a suppression by a factor of five for these hadrons. The observed suppression can be viewed as a modification of the fragmentation functions of quarks and gluons due to the surrounding medium. The detailed interpretation of these results is discussed in Section 3.2.

One method for isolating quark jets (as opposed to gluon jets) is to look for D and B mesons that predominantly come from the fragmentation of charm and beauty quarks. Because of their large mass M these heavy quarks are produced early (on a time scale $1/2M$) and later production by thermal processes is strongly suppressed. There are two methods of measuring heavy flavor mesons at RHIC. Direct D meson reconstruction is presently limited to low p_T , but gives useful information on the scaling of the total charm cross section (150). These results are consistent with binary collision scaling of total charm production, but still have large errors. Since charm, once created, is unlikely to be annihilated, we expect the total number of c and \bar{c} quarks to remain constant after their initial production. The second method involving the measurement of “non-photonic” electrons has proven to be extremely useful at RHIC. Results from the PHENIX and STAR experiment give yields for these electrons in proton-proton through central gold-gold collisions over a wide p_T range. They indicate a significant suppression $R_{AA} \ll 1$ in central gold-gold reactions (151).

This suppression came as a surprise, because expectations were for a reduced energy loss for heavy quarks than for light quarks fragmenting into pions and other light hadrons. In the theoretical framework of parton energy loss via gluon radiation, this expectation is for two reasons. First, the D meson almost always derives from a charm quark, but the pion spectrum has contributions from quark

and gluon fragmentation, and the energy loss of gluons is expected to be about twice that of quarks. Second, the more massive charm quark should suffer a “dead-cone” effect suppressing the forward emission of gluons (88). The strong suppression of heavy meson production has led to a re-assessment of alternative scenarios of parton energy loss, and is discussed in Section 3.2.

Measurements of jet quenching phenomena at RHIC are not restricted to single particle yields. Since fragmenting partons are the result of hard parton-parton scattering processes, they should be accompanied by a partner jet at the opposite azimuthal angle. The RHIC experiments are not capable of complete jet reconstruction in heavy ion reactions due to the modest $p_T < 25$ GeV of the jets and the large background of uncorrelated low p_T particles in central gold-gold collisions. Instead, experiments correlate identified hadrons in momentum space. The STAR and PHENIX experiments have shown analyses that use the highest p_T hadron as the trigger particle, defining azimuthal angle $\phi = 0$, and then plot $\Delta\phi$ with other hadrons (associated particles) in the same event. In proton-proton reactions this analysis results in a sharp peak centered at $\Delta\phi = 0$, due to other hadrons fragmenting from the same parton as the trigger particle, and a wider peak near $\Delta\phi = \pi$, due to hadrons fragmenting from the opposing parton.

However, in gold-gold reactions, first results from the STAR experiment triggering on a high p_T particle and correlating it with associated hadrons with $p_T > 2$ GeV/c showed the complete disappearance of the opposite side peak (152), as shown in Figure 9. Energy and momentum must be conserved globally, implying that particles from the opposing parton must either be shifted to lower energy ($p_T < 2$ GeV/c) and/or be scattered into a diffuse angular distribution. New results from higher statistics gold-gold data reveal that both effects are significant (153). In lowering the required p_T for associated particles to 200 MeV/c, one recovers the energy of the opposing parton. Remarkably these particles are spread out over nearly the entire opposite side hemisphere ($|\Delta\phi| > \pi/2$) and with a mean $\langle p_T \rangle$ not much larger than the average p_T of all other particles emitted from the medium (103). The data may indicate that the peak of the backward angular distribution is no longer at $\Delta\phi = \pi$, but near $\Delta\phi \approx 2\pi/3$ (154), shown in the lower panel of Figure 9. The experiments have embarked on measuring three- and more-particle correlations in order to understand the emission of these associated particles in detail.

A different probe of the medium comes from quark-antiquark pairs rather than just single partons. The possible suppression of heavy quarkonia (J/ψ , χ_c , ψ' , Υ) due to color screening – analogous to Debye screening in an electromagnetic plasma – has long been proposed as a probe of deconfinement (155). Like in the case of jets, the usefulness of heavy quark bound states as probes of dense matter must be calibrated against their behavior in proton-nucleus or deuteron-nucleus reactions. Measurements of the absorption of J/ψ in deuteron-gold reactions by the PHENIX experiment indicate that the state has a break-up cross section with nucleons in the gold nucleus of order 1 – 3 mb (156). Note that at this energy the gold nucleus sweeps over the quark-antiquark pair on a time scale of $2R/\gamma c \approx 0.14$ fm/c, i. e. before the bound state has been formed.

Results from the PHENIX experiment in copper-copper and gold-gold reactions reveal a suppression of J/ψ yields relative to binary scaling expectations (157). The suppression appears to be greater than can be accounted for by break-up from the two gold nuclei passing through, thus leaving some room for additional suppression in the medium created. However, the level of suppression is not very

different from that observed at lower energies by the NA50 experiment at the CERN-SPS (158). Model calculations assuming color screening of the J/ψ state in medium predicted a much larger suppression at RHIC energies due to the larger parton density, higher temperature, and longer lifetime of the system (42). One possible explanation is that the color force responsible for binding the J/ψ is in fact not strongly screened in the medium, as recent lattice results suggest (43). Another possibility is that one forms additional J/ψ later in the reaction from the coalescence of $c\bar{c}$ quark pairs or hadronically via $D\bar{D} \rightarrow c\bar{c}$ reactions (159). Future detailed measurements of open charm and quarkonia are required to discriminate between these various scenarios.

3 Interpretation of Results

3.1 The "ideal fluid"

As we discussed in Section 2.2, the "elliptic flow" parameter v_2 characterizing the azimuthal anisotropy of the hadronic spectra depends on the hadron species and exhibits an almost linear dependence on the transverse momentum p_T . The strong p_T -dependence suggests that this cannot be a simple consequence of the geometric aspect ratio of the emitting source (160). The strong dependence of the magnitude of v_2 on the hadron mass for small p_T , which nicely matches the predictions of fluid dynamical simulations of the expansion of an ellipsoidal fireball (161), suggests that v_2 is the result of an anisotropic expansion caused by the difference in pressure gradient in and out of the collision plane. This does not mean that other effects, such as an angular dependence of absorption, can be entirely neglected, but they are subdominant in the bulk emission region ($p_T < 1$ GeV/c) (162).

The generally good agreement between the $v_2(p_T)$ curves expected from the collective expansion of an ellipsoidal fireball and the measured v_2 curves for a variety of hadrons makes it worthwhile asking to which aspects of the expansion they are sensitive. The most obvious details are: the initial conditions, the equation of state, and the viscosity of the expanding matter. The formation of a collective flow velocity in an inviscid fluid is governed by the relativistic Euler equation

$$\frac{d}{dt}(\varepsilon\vec{v}) = -\nabla P, \quad (6)$$

implying that the formation of collective flow relies on the existence of a pressure gradient. Elliptic flow requires the existence of an azimuthally anisotropic pressure gradient. Since transverse expansion quickly reduces any initially existing anisotropy of this kind, it can be shown that a substantial elliptic flow in non-central collisions must be formed during the early stages of the fireball evolution (163). It hence requires the rapid formation (< 2 fm/c) of a large pressure by equilibration.

Quantitative solutions of relativistic fluid dynamics confirm this expectation. The elliptic flow is generated mainly during the first 5 fm/c of the expansion, and the pressure gradient has to become active before 1 fm/c (164). These results imply that the observed elliptic flow is generated when the energy density of the matter exceeds 1 GeV/fm³. The calculations also show a sensitivity to the equation of state, but no consensus has been reached yet as to how well the $\varepsilon(P)$ relation can be determined in this way (163, 165, 166).

A nonvanishing viscosity modifies the right-hand side of (6) and thus affects the generation of elliptic flow. Numerical solutions of the relativistic Navier-Stokes equations have shown that even a low (but non-zero) shear viscosity η has a dramatic effect on the value of v_2 generated during the expansion (167). The approximations and idealizations necessary presently preclude a precise determination of an upper limit for η compatible with the elliptic flow data, but it seems safe to conclude that the condition $\eta/s \ll 1$ must hold.

One problem arising when one tries to pin down the equation of state by a comparison between the data (p_T spectra and v_2 and the space-time information from two-particle-correlations) and the results of hydrodynamic calculations is that it is difficult to obtain a good description of all data simultaneously. In part, this problem arises from the failure of fluid dynamics to provide for an accurate description of the expansion during the final, hadronic gas phase (168). The hadron gas has a rather large viscosity and also fails to maintain chemical equilibrium during the cooling period until particle freezeout occurs. Hybrid descriptions in terms of fluid dynamics for the deconfined phase followed by a Boltzmann cascade for the hadronic phase will make it possible to address this issue (169, 170).

An important source of information about the collective flow comes from the spectra and angular distributions of heavy mesons. Originally, heavy quarks were not expected to participate in the collective flow to a significant degree, but this expectation has been revised in view of the observed strong suppression of hadrons containing heavy quarks at large p_T (see Section 2.3). A large energy loss requires large cross sections for heavy quarks in the medium. One would then also expect the heavy quarks to more fully reflect the global flow of the medium. Because their production is a hard process even at moderate momentum, heavy quarks may become more controlled probes of the pre-hadronic collective flow than hadrons composed solely of light quarks (171, 172). The large mass of heavy quarks may also allow for a more rigorous description of the hadronization process and thus make quantitative tests of quark recombination models possible (173). We will return to the transport properties of heavy quarks in the medium in Section 3.2.

3.2 Energy loss jet tomography

As explained in Section 1.2, the energy loss of a light parton in dense matter is controlled by a transport coefficient \hat{q} , which is proportional to the density of color charges in the medium. The value of \hat{q} can be calculated in pQCD, where it is found to scale like a power of the energy density $\hat{q} = c\varepsilon^{3/4}$ with $c \approx 2$ independent of the temperature, and even holding for cold nuclear matter (174). However, the analysis of the RHIC jet quenching data, assuming a thermal quark-gluon plasma and the boost invariant Bjorken scenario, yields a much larger value, corresponding to $c_{\text{exp}} \approx 10$ (86). If this analysis is correct, it implies a five times shorter mean free path for hard partons than is predicted by perturbation theory. One can view this result as a confirmation of the conclusion described above, that the viscosity of the medium must be very low, because that also implies a very short mean free path for thermal particles.

A slightly different analysis of the jet quenching data assumes that the energy loss can be described perturbatively and uses the data to deduce the density of scattering centers in the medium. If these are all assumed to be gluons, the data

require a density dN_g/dy of 1000 – 1200 per unit rapidity (175,176). It is notable that these calculations do not imply that the medium constituents are objects with open color (e.g. gluons). In deep inelastic scattering reactions the photon can scatter from individual quarks if its virtuality is such that its wavelength is shorter than the size of the proton (about 1 fm). Similarly, the hard scattered parton could resolve color charges within the constituents of the medium, even if these objects were color singlets, such as hadrons.

As discussed earlier, radiative energy loss is less effective for heavy quarks than for light quarks and gluons. As a result, calculations (178) show that the suppression of mesons with charm should be only about half as strong as the suppression of light mesons in the range $p_T < 10$ GeV/c. The suppression of B -mesons in this range is even smaller, $R_{AA}^{(B)} > 0.8$, if realistic gluon densities in the medium are assumed. These results are in strong disagreement with the data on “non-photonic” electrons.

One possible resolution of this quandary is the realization that collisional energy loss is important for heavy quarks (179), triggering a re-evaluation of its importance for light quarks and gluons as well. Since the scattering centers in the medium are not infinitely massive, a hard parton loses energy even in an elastic collision. Because the energy loss per collision is small, but the parton suffers many collisions in the medium if its mean free path is small, the collisional energy loss can be described by a Langevin equation in which the diffusion coefficient D is an adjustable parameter (180). In order to achieve reasonable descriptions simultaneously for the “non-photonic” electron R_{AA} and v_2 , one needs a diffusion constant in the range $3 < 2\pi TD < 6$, which corresponds to a very small shear viscosity $1 < 4\pi(\eta/s) < 2$. Such a small diffusion constant near the conjectured absolute lower bound (22) is difficult to reconcile with perturbation theory. One possible explanation of a large charm energy loss would be the presence of D -meson like resonances in the medium above T_c (181).

Recently a study including both, radiative and collisional energy loss, has been made which includes effects of the collision geometry as well as path length fluctuations (182). The study uses perturbative cross sections and assumes a density of gluons in the medium. The authors conclude that the two effects combine to explain the observed R_{AA} for light and heavy mesons simultaneously for a realistic gluon density $dN_g/dy \approx 1000$.

One problem with these estimates is that they assume that the quark-gluon plasma is predominantly composed of gluons. If the medium is chemically equilibrated, it contains a substantial fraction of quarks and antiquarks, which have smaller perturbative cross sections than gluons. The required rapidity density then rises to about $dN_{qg}/dy = 2000$. The problem with this result is that it is incompatible with the final entropy density $dS/dy \approx 5000$ deduced from the measured charged hadron multiplicity (177). The entropy density at early times cannot be less, putting a limit $dN_{qg}/dy \leq \frac{1}{4}dS/dy \approx 1300$. This argument again suggests that the parton-parton cross sections in the medium must be significantly larger than predicted by perturbation theory.

3.3 Thermodynamic properties

The RHIC data constrain the thermodynamic properties of the matter produced in Au+Au collisions, such as its entropy density. The total final-state entropy can be deduced either from the measured hadron yields in combination with

information on the size of the emission volume, or from the implied hadron yields at chemical freeze-out assuming full chemical equilibration. The first of these methods starts from the expression for the entropy in terms of the phase-space distribution $f_i(x, p)$ of non-interacting particles (i denotes the particle species, d_i its degeneracy):

$$S = \sum_i d_i \int \frac{d^3x d^3p}{(2\pi)^3} [-f_i \ln f_i \pm (1 \pm f_i) \ln(1 \pm f_i)], \quad (7)$$

where the $+(-)$ sign holds for bosons (fermions). The momentum dependence of the functions $f_i(x, p)$ is determined from the measured or fitted p_T spectra. The spatial x -dependence is assumed to be Gaussian, with radii fitted to the two-particle correlations using the Hanbury-Brown-Twiss (HBT) effect. This approach yields a final entropy per unit rapidity at $y \approx 0$ of $dS_f/dy \approx 4450$ for the 11% most central Au+Au events at $\sqrt{s_{NN}} = 130$ GeV (177). This number scales to $dS_f/dy \approx 5600$ at midrapidity in the 6% most central events for the highest RHIC energy ($\sqrt{s_{NN}} = 200$ GeV).

The second method starts from the entropy per particle $S/N = 7.25$ of a fully equilibrated hadronic resonance gas at the chemical freeze-out temperature $T_{\text{chem}} \approx 170$ MeV (183). Using the fit of hadron yield ratios and the total measured charge multiplicity, one can deduce an entropy content of $dS_{\text{chem}}/dy \approx 5100$ at chemical freeze-out (184). Since the cooling from T_{chem} until final decoupling of all hadrons at $T_f \approx 110$ MeV proceeds through the rather viscous hadronic gas phase, the implied increase of the entropy by 10% between chemical and kinetic freeze-out is realistic (168). On the other hand, as discussed in Section 3.3, the collective flow analysis tells us that the viscosity at even earlier times must be very small. We can thus conclude from the RHIC data that the entropy during the hydrodynamic expansion of the matter at temperatures $T > T_c$ is $dS/dy \approx 5000$ with an estimated error of ± 400 . In the framework of three-dimensional relativistic fluid dynamics, this result can be used to obtain estimates of the evolution of the entropy density of the matter between the moment of first equilibration and the transition into a hadronic gas at T_c . Assuming a boost invariant longitudinal expansion and averaging over the transverse plane, one obtains an entropy density of about $33/\text{fm}^3$ at a time of 1 fm/c (184), corresponding to a temperature of 270 MeV for 30 massless degrees of freedom. This estimate assumes that the entropy growth during the “ideal liquid” phase of the medium is negligible.

It thus appears that a rather precise determination of the entropy density of the hot medium at early times with an uncertainty in the range of $(5 - 10)\%$ is within reach, once an analysis without the assumption of boost invariance has been performed. If it were possible to obtain a similarly accurate measurement of the energy density, from jet quenching data or other considerations, this would enable a model independent determination of the equation of state (184), which could be compared with the lattice predictions. In particular, it would allow for a determination of the effective number of (massless) degrees of freedom in the medium. Lattice QCD predicts that this number rises steeply near T_c , but then remains almost constant over a wide temperature range. This prediction could then be tested by comparing results obtained at widely different beam energies.

3.4 Partonic collectivity

Perhaps the most direct source of evidence for the nature of the matter produced at RHIC is derived from the recombination model of hadron production at intermediate $p_T = 2 - 5$ GeV/c (141, 185–187). In this model, which gives successful descriptions of measured hadron yields and v_2 in terms of an underlying thermal valence quark spectrum, the primary constituents of the medium just prior to hadron emission have the quantum numbers of quarks and antiquarks in complete chemical equilibration. The theoretical argument for rapid flavor equilibration of u, d, s quarks is based on the abundance and large cross section of thermal gluons at temperatures above T_c in perturbative QCD (188). This expectation is confirmed by the near perfect flavor equilibration of the emitted hadrons. However, this raises the question: what happens to the thermal gluons as the system cools through T_c ?

In part, the answer may be that the gluons get incorporated into the emitted hadrons. In the recombination model, one can show that the emission probability of a hadron from a thermal medium does not depend on details of its internal wave function (189). If the wave function contains higher Fock states including additional gluons besides the valence quark configuration, the emission process can absorb some of the gluons in the medium. However, the internal structure of the emitted hadrons does have an influence on the valence quark scaling law for the v_2 component of the collective flow. Components of the hadron wave function containing additional gluons or sea quarks lead to deviations from the naive scaling law in the few percent range which could be detected by precise measurements.

A great deal of the uncertainty in our understanding of the process of hadronization is rooted in our lack of precise knowledge of the structure of the quark-gluon plasma in the temperature region just above T_c . Various results from the lattice, as well as the RHIC data, indicate that it is a strongly coupled state. As we briefly mentioned in Section 1.2, it is possible to use lattice results for the susceptibilities of various quark flavor related quantities, such as strangeness, electric charge, and baryon number, to conclude that the excitations of the matter just above T_c have the quantum numbers of individual quarks, not diquarks or quark-antiquark pairs (27, 28). The analysis shows that the transition from a medium dominated by meson ($q\bar{q}$) and baryon ($qqq, \bar{q}\bar{q}\bar{q}$) bound states to quark-like states occurs rapidly and completely when the temperature exceeds T_c (190). The best way to test this regime may be with hadrons containing heavy quarks, for which the hadronization process is much better understood (see e. g. (173)).

4 Outlook

4.1 Review of lower energy results

There have been two previous experimental programs with relativistic heavy ion collisions at energies sufficient to consider the possible formation of a quark-gluon plasma. Both were fixed target programs. One used the Alternating Gradient Synchrotron (AGS) at Brookhaven National Laboratory to accelerate heavy ion species up to gold nuclei and center-of-mass energies per nucleon pair in the range $\sqrt{s_{NN}} = 2.4 - 4.8$ GeV and the other the Super Proton Synchrotron (SPS) at CERN with species up to lead nuclei with $\sqrt{s_{NN}} = 7.6 - 17.3$ GeV.

The BNL-AGS program resulted in strong evidence for the creation of “resonance matter” where most all hadrons are in excited states cascading and decaying into stable hadrons (191). The possibility of modest temperature and finite baryon density quark-gluon plasma formation in the very short earliest stages is not ruled out, but the program lacked measurements of penetrating probes of these early time stages. Intriguing results such as enhanced $\bar{\Lambda}/\bar{p}$ persist (192), but are currently unexplained.

The CERN-SPS program had a broader suite of experimental observables and was at significantly higher collision energy. In the year 2000, there was a CERN press release announcing “evidence for a new state of matter” In evaluating the experimental evidence they concluded that “the new state of matter found in heavy ion collisions at the SPS features many of the characteristics of the theoretically predicted quark-gluon plasma” (193).⁷ It is notable that the document describes the quark-gluon plasma as a state where “quarks and gluons... freely roam within the volume of the fireball”.⁸ The argument placed significant weight on the “strong nonlinear dependence” of the enhancement of multi-strange hadrons and the suppression pattern of charmonium states where “intermediate $c\bar{c}$ seems to disappear quite suddenly in semicentral lead-lead collisions, and in the most central lead-lead collisions an additional reduction of the J/ψ ” is observed.

Over the past five years, changes in the experimental data and theoretical understanding have tempered some of these conclusions. First, it is quite unlikely that at CERN-SPS energies or even at RHIC, the quarks and gluons should “roam freely.” While quarks and gluons are most likely liberated from their hadronic bonds, they are still strongly interacting in the medium with mean free paths less than 1 fm. Second, the concept of “sudden” observed transitions as a function of energy density is recognized as unnatural even in the case of a first-order phase transition, where observables exhibit discontinuities as function of temperature, but not as function of the energy density. Given the evidence for a smooth cross-over transition from lattice calculations, such discontinuities appear highly unlikely. Indeed, the experimental evidence for “non-monotonic derivatives” in the suppression of $\bar{c}c$ states (195) has not held up to further scrutiny, and strangeness enhancement appears to have a gradual onset with significant effects already seen in proton-nucleus reactions (196, 197).

Nonetheless, these lower energy fixed target programs provided major advances in the field. Many of the experimental observations still challenge our theoretical framework and emphasize the importance of measuring the excitation function (collision energy dependence) of many observables from the AGS to the CERN-SPS to RHIC and, in the future, to even higher energies in the LHC heavy ion program. Not only is the excitation function of interest, there is unique physics at these lower energies. The CERN-SPS program on heavy quarks and low mass dileptons has been revived with the NA60 experiment (198). The NA49 experiment has mapped out hadronic observables over the complete energy range between the BNL-AGS and the top CERN-SPS energy (199), and the NA45 experiment has focussed on low mass dileptons and also higher p_T hadrons (200). At these lower energies, matter at the highest net baryon density will be studied with precision experiments at the planned FAIR facility at GSI (201). Although

⁷Since there was no peer-reviewed publication associated with this announcement, we refer here to the document that accompanied the press release.

⁸The authors have clarified (194) that “roaming” was not intended to mean moving without interactions.

at RHIC the transition to a QGP appears to be a smooth cross-over, there may exist a tri-critical point in the phase diagram at large net baryon density where the transition changes to first order. These lower energy programs have a unique opportunity to study this region of the phase diagram of nuclear matter.

4.2 Future outlook for RHIC

The great progress in characterizing and understanding the medium created at RHIC over the past five years invites the question of what are the critical outstanding issues and key additional measurements needed to further characterize the properties of the quark-gluon plasma.

The four experiments have made an almost complete determination of the global features of the medium and its collective motion at $\sqrt{s_{NN}} = 200$ GeV.⁹ The main experimental thrust of the future will be in the area of hard and rare probes with low cross section or small branching fractions, which require an increased luminosity and enhanced detection capabilities.

In order to better dissect the mechanism responsible for jet quenching and more accurately determine the color charge density in the medium, we want to distinguish quarks traversing the medium from gluons. The color octet gluons should lose energy at roughly twice the rate as the color triplet quarks. The present measurements of high p_T hadron suppression cannot separate contributions from quark and gluon fragmentation, and the standard techniques used to isolate gluon jets via 3-jet event analysis do not work for modest p_T jets in the high background of nucleus-nucleus collisions at the RHIC beam energy. In the future, RHIC experiments will use identified hadrons to separate these jet contributions on a statistical basis. One prediction is that the \bar{p}/p ratio should drop at high p_T since antiprotons are statistically more likely to originate from a gluon initiated jet, which should lose more energy in the medium.

An alternative method of separating quark jets is by tagging charm and beauty mesons at high p_T , where they are almost exclusively fragmentation products of heavy quarks. Both PHENIX and STAR have proposed upgrades including inner silicon detectors to measure displaced vertices from these heavy flavor decays. Not only does this tag quark jets, but also allows for the study of the “dead cone” effect due to their finite velocity if radiation is the dominant energy loss mechanism. Direct reconstruction of charm mesons and baryon states, tagging single electrons from D and B meson decays, and tagging J/ψ from B decays will give experiments many handles on this physics.

Further details can be gleaned by studying γ -jet correlations since the photon tags the jet energy at leading order in α_s . This method requires higher beam luminosity, which can be achieved through an accelerator upgrade including electron cooling of the gold ion beams.

As previously shown in Figure 9, there is strong evidence from STAR and PHENIX that partons propagating through the medium have a fragmentation pattern showing an increased yield of hadrons at low p_T and a very broad angular distribution. The possible two-peaked structure in the angular distribution and the correlation of this structure with modification in the $\langle p_T \rangle$ have led to much speculation about the response of the medium to the deposited energy.

⁹It should be noted that this level of detailed measurement remains to be completed at lower energies all the way down to RHIC injection energy, where one can make direct comparisons to the fixed target CERN-SPS results.

It is possible that this response takes the form of a Mach cone of sound waves (219,220), or a wake in the color fields (218), or is the result of gluonic Cherenkov radiation due to an elevated index of (gluon) refraction of the medium (221,222). The detailed measurement of identified multi-particle jet correlations may help distinguish between these scenarios. These analyses require very high statistics which will be available after the luminosity upgrade.

The heavy quarkonia program at RHIC has just started. Additional upgrades to detectors and improvements in luminosity are needed to fully quantify the level of suppression in heavy ion reactions relative to proton-proton and proton-gold or deuteron-gold reactions over a wide kinematic range. In addition, measurements of the different quarkonia states are important for determining whether the suppression relates to color screening or to collisional interactions with other partons. The lattice results for spectral functions in the quenched approximation suggest that measurements of the less strongly bound χ_c states should be a focus of the program. The deeply bound $\Upsilon(1s)$ is also interesting, because it may be unaffected by the medium if the temperature reached at RHIC is not much above T_c . Additional data on open charm yields and flow will help confirm or refute models predicting large J/ψ formation from initially uncorrelated c and \bar{c} via recombination.

Recent preliminary results from the NA60 experiment (198) at the CERN-SPS have confirmed the earlier NA45 results (202) of a low-mass enhancement in dilepton production below the $\rho(770)$ mass. The excellent resolution and precision of these new results has reignited hopes that measurements of the dilepton spectrum will permit a determination of the modification of the ρ spectral function in the medium and, indirectly, yield evidence for the gradual restoration of chiral symmetry upon approach to T_c . These measurements are extremely challenging at RHIC as the backgrounds are very large. Upgrades for the PHENIX experiment with a hadron blind detector and improved Dalitz rejection using time of flight and micro-vertex detection in the STAR experiment will make these measurements possible.

One can also measure thermal radiation with direct or virtual photons. Again, there is large background from π^0 and η decays, but the rewards for successful efforts are great. A measurement of the thermal temperature of the medium is a critical step towards detailing the number of active degrees of freedom in the equation of state. PHENIX has recently introduced a new analysis technique for heavy ions by measuring virtual photons via e^+e^- pairs and then subtracting the hadron decay contributions by studying the invariant mass distribution of the pairs (154). Additionally the measurement of $\gamma\gamma$ HBT correlations (203) to eliminate these decay contributions may help to constrain the time evolution of the temperature.

4.3 Outlook for LHC program

In the very near future, the Large Hadron Collider (LHC) at CERN will be commissioned for high energy proton-proton and heavy ion lead-lead reactions. These heavy ion collisions will be at a center-of-mass energy of 5.5 TeV per nucleon pair, thus bringing 1144 TeV in total kinetic energy into collision. A detailed overview of the program is given in (204). There are three experiments that will collect data during heavy ion running: ALICE, ATLAS and CMS. The ALICE experiment is a detector system dedicated to heavy ion physics with

capabilities designed for the characterization of the quark-gluon plasma. The requirements include large coverage to low transverse momentum, excellent particle identification, and specialized detectors for specific channels of interest (for example $J/\psi, \Upsilon \rightarrow l^+l^-$). ATLAS and CMS are detectors primarily designed for discovering the Higgs boson, supersymmetric particles, and other new physics. Both detectors have excellent calorimetry with large coverage and inner silicon detectors for charged particle tracking. Thus, the experimental program at the LHC is well equipped, and despite only one month of heavy ion running per year, the large rate capabilities of these detectors make the program very promising.

It is possible that at the LHC one will achieve energy densities such that a weakly interacting quark-gluon plasma is formed, because thermal interactions are of sufficiently large q^2 that $\alpha_s \ll 1$. This would be extremely interesting as one would see the perturbative calculations which have failed to describe data at RHIC then becoming applicable at the LHC. Such a scenario could imply, for instance, that the elliptic flow v_2 at LHC may be smaller than at RHIC energies. It is also possible that the quark-gluon plasma at LHC energies will still be a strongly interacting system for most of the medium's time evolution.

Another exciting part of the program at the LHC is that the gluon density in the incoming nuclei is much higher than at RHIC. Thus, studies of saturation physics will enter a new regime at the LHC. Additionally, measurements of $\gamma + jet$ events at forward angles will allow precise kinematic determination of the initiating partons (x_1, x_2), and thus will allow for precise measurements of deviations from predictions based on factorized parton distributions.

The higher energies of the LHC not only imply a higher initial temperature, but also that even higher q^2 probes of the medium are available and abundantly produced. Quark and gluon jets will be measurable well above $p_T > 200 \text{ GeV}$. In addition, the tagging of heavy flavor jets from displaced vertices is possible in all three experiments. At these very high p_T the interactions with the medium are expected to be completely dominated by induced gluon radiation and describable by pQCD. Quarkonia studies will also benefit from the higher energy as abundant production of the $\Upsilon(1s, 2s, 3s)$ states will allow detailed studies of these bound states.

The RHIC and LHC programs should prove to be quite complementary whether it turns out that LHC induced collisions are in the strongly coupled or weakly coupled regimes or somewhere in between.

4.4 Open theoretical problems

The main unsolved theoretical problems concerning nuclear collisions at RHIC fall into five classes:

1. Understanding the mechanisms behind early equilibration and thermalization, and entropy production, in general;
2. The microscopic structure of the quark-gluon plasma in the temperature region above, but not far above, T_c ;
3. The numerical solution of three-dimensional, viscous relativistic fluid dynamics;
4. The effect of localized energy deposition by a hard parton on the medium.
5. The process of bulk hadronization.

This does not mean that there are not many other interesting and important theoretical problems, but these generally can be approached in a now well established framework. What distinguishes the five issues listed above is that the framework, in which they can be addressed, is still uncertain. Thus, all we can do here is to describe some ideas that hold promise for future studies.

Equilibration: The most promising conceptual framework for a rigorous treatment of parton equilibration on the basis of QCD currently is the idea that nuclear matter is transformed in the collision from saturated gluonic matter in a universal quantum state (the color glass condensate) to a thermalized and equilibrated quark-gluon plasma (205). The theoretical arguments for this scenario invoke asymptotically high beam energies; whether this condition already applies in the energy domain at RHIC, remains to be seen. Three steps can be distinguished in this process: the decoherence of the initial quasi-classical quantum state into particle-like quanta; the approach to local isotropy of the resulting parton distribution; finally, thermalization and chemical equilibration.

The decoherence of the initial state has so far been studied mostly by means of numerical solution of the Yang-Mills equations (206–208). These simulations do not, however, answer the question how entropy is created in this process. A recent attempt to estimate the decoherence time by analytical techniques gives a value of the order of $Q_s^{-1} \sim 0.2 \text{ fm}/c$ (209). The entropy created solely by the decoherence (“shattering”) of the color glass condensate can be estimated to be about 1/3 of the finally observed entropy (210).

A promising mechanism to explain the apparent early isotropization of the distribution of liberated partons are the instabilities which generically exist in a parton plasma with an anisotropic momentum distribution (60). These lead to the exponential growth of coherent color fields, dominantly of color-magnetic nature, which can efficiently deflect partons. It is not clear at present whether these fields can also speed up complete thermalization (62), for example by enhancing gluon radiation via synchrotron-like emission of soft quanta (211). Since the longitudinal expansion of the matter, which persists even at late times, continually acts as a driver of a momentum space anisotropy in the parton distribution, coherent fields due to plasma instabilities may well remain present in the medium at all times, as long as the temperature exceeds T_c . They may thus be a part of the structure of the matter that we are studying experimentally, rather than just a mechanism for its equilibration.

Structure of the quark-gluon plasma: A detailed insight into the microscopic structure of thermal QCD matter in the region $T_c \leq T \leq 2T_c$ is of utmost importance for our understanding of the physics of most experimental probes. In principle, the tool for the theoretical investigation of this structure exists: lattice gauge theory. A problem is that it is not sufficient to calculate various quantities on the lattice; one must also be able to extract a physical picture from the lattice results. Such studies usually proceed in various levels of sophistication: from global properties, such as the equation of state, over various susceptibilities describing fluctuations around the equilibrium state and static correlation functions, to dynamical correlations and spectral functions. High quality lattice results now exist for the equation of state, susceptibilities and many static correlators, but a systematic analysis of these results in terms of physical models is still in progress. The calculations of spectral functions on the lattice are still in their infancy and presently restricted to calculations without dynamical quarks. This greatly limits their usefulness at the present time.

The recent progress in solving strongly coupled supersymmetric gauge theories by means of duality techniques is another very promising approach (see (212) for a recent review). One problem here is that the connection between the degrees of freedom in the gauge theory at weak and strong coupling is not well understood, making it difficult to model the transition between the two regimes. Another hurdle is that it is difficult to formulate supersymmetric gauge theories on the lattice (213) and study them across the entire range of coupling constants. Another possible approach to study the structure of the quark-gluon plasma away from weak coupling is molecular dynamics (214, 215).

Viscous 3-D fluid dynamics: The RHIC data clearly demonstrate that the medium produced in nuclear collisions is not boost invariant. A realistic treatment of the reaction therefore requires full solutions of relativistic fluid dynamics in three dimensions. Such solutions have recently become available, including hadronic cascade treatments of the break-up phase (170, 216, 217). An important missing aspect of these solutions is the presence of a physical viscosity. Although the data suggest that the viscosity should be small in the plasma phase, full three-dimensional (numerical) solutions of viscous, relativistic hydrodynamics for a given equation of state and realistic initial conditions are needed in order to deduce an upper limit of the viscosity from the collective flow data.

Medium response to energy deposition: The current interest in this problem is driven by the experimental observations of an enhancement of soft hadron emission over a wide angular range in association with a recoiling energetic hadron. The theoretical problem here is presumably quite well defined: What is the response of the thermal medium to a color charge that propagates through it at nearly the speed of light (218)? The problem is complicated by the fact that the color charge itself evolves on its way through the plasma due to scattering and radiation. It is an interesting question whether a scale exists that separates the evolution of the propagating charge from the response of the medium. Of course, one needs to bear in mind that, even if such a scale exists in principle, the energies accessible at RHIC may not be sufficiently high for its application. Present models suggest that an explanation of the data in terms of a Mach (218–220) or Cherenkov (221, 222) cone requires an extremely efficient coupling between the color field of the penetrating parton and the collective modes of the medium (223). Studies of possible mechanisms for this coupling, either by perturbative techniques or molecular dynamics simulations, will be important.

Bulk hadronization: The competition of hadronization in bulk with the fragmentation mechanism familiar from jet formation was proposed early on as a signature of the formation of a deconfined quark-gluon plasma (224). But before the advent of RHIC, the kinematic range of transverse momenta p_T where this competition can be studied was inaccessible. As discussed in Section 3.4, the thermal recombination model explains some of the more surprising features of hadron production observed in the RHIC experiments. The persistence of di-hadron correlations (225, 226) in the p_T -domain where recombination appears to dominate over vacuum fragmentation indicates that either recombination processes involving both, hard scattered and thermal partons (227), or local momentum correlations in the hadronizing medium (228) are important. This suggests the need for a theoretical framework that treats fragmentation and recombination as two limiting cases of a unified hadronization scheme. First steps in this direction have recently been taken (229).

5 Summary

Relativistic heavy ion physics has witnessed several paradigm shifts during the past decade driven largely by experimental discoveries. The power of large, multipurpose detectors suited to the simultaneous measurement of many observables has also been demonstrated. As a result of these innovations and the availability of a dedicated accelerator facility, RHIC, much progress has been made in a relatively short time.

In Section 1.2 we stated that the experimental quest for the quark-gluon plasma must proceed in steps: First, the determination that the particles produced in the nuclear reaction really form, for a brief period, matter that deserves a description in thermodynamic terms; second, the determination that this matter has a novel structure and is not just a dense gas of hadrons; and third, the characterization of its main physical properties. At the time of this review, the first two steps have clearly been achieved. We are confident that the matter has been thermodynamically equilibrated, probably at an early time in the reaction, and we have found compelling evidence for the case that the structure of this matter is different from any known before. The third step, involving the characterization of its properties by systematic experimental investigation, is in progress. In order to succeed, it will require improvements in the RHIC detectors and a substantial increase in the available luminosity.

On the theory side, the original expectation that the quark-gluon plasma would be a “simple” state of matter characterized by largely perturbative interactions and transport processes has fallen by the wayside. It has been replaced with the understanding that the quark-gluon plasma, at least in the parameter regime accessible at RHIC, is a state of matter characterized by strong interactions among its constituents and by novel properties, such as a very low viscosity and large stopping power. This insight is not entirely new; the temperature region near T_c was always recognized as one for which calculations are hard and quantitative predictions difficult. The results from RHIC have forced theorists to face these difficulties.

No consensus has yet emerged about what the microscopic structure of this new state is, but we do have an ever improving tool - lattice gauge theory - that allows us to determine some of its properties in a model independent way. One of the results obtained in this way is the equation of state and the recognition that it does not contain a strong discontinuity, such as a first-order phase transition, under the conditions (approximately vanishing net baryon number density) prevailing at RHIC. This insight, in turn, has done away with the previously held expectations of discontinuities in experimental data as function of beam energy, impact parameter, or nuclear size. Any changes observed as function of these parameters must be continuous, even though it may be rapid, as the transition from hadronic matter to a quark-gluon plasma takes place.

Perhaps the most basic insight from the RHIC data is that nearly thermalized matter is, indeed, produced in nuclear collisions. In fact, the ensemble of emitted hadrons is so well thermalized, both kinetically and chemically, that one has to look at rare probes, such as unstable resonances or hadrons emitted at high transverse momentum, to find deviations from equilibrium. These results leave us quite confident that matter, in the thermodynamic sense, is being produced. The large collective transverse flow, which shows a quadrupole anisotropy in noncentral collisions, signals that the equilibration happens very early in the

reaction, probably at time less than 1 fm/c. This conclusion relies on comparisons with solutions of relativistic fluid dynamics, which can be made to agree well with the data for realistic equations of state. Calculations using viscous fluid dynamics, with certain somewhat questionable approximations, lead to an even stronger conclusion: that the matter must be nearly inviscid, a nearly “perfect” fluid, and the mean free paths of particles in it must be very short.

The other important new insight is that the medium produced in nuclear collisions has a large opacity to energetic particles carrying a color charge. The numbers extracted from the RHIC data push the limits of possible explanations within the perturbative theory of energy loss for light partons in QCD, and they clearly exceed them for heavy quarks. Again, the mean free path must be shorter than expected in a perturbative framework. The stopping power of the medium makes much more detailed measurements of jet quenching possible at RHIC than was anticipated, and “jet tomography” has become an important experimental tool for the characterization of the medium, its geometry, and its evolution.

This summary would be incomplete without mentioning that not all data measured in nuclear collisions are well explained and understood. A prime example are the measurements of identical particle correlation functions, which do not agree with the predictions of fluid dynamical calculations that fit the hadron spectra. It may well be that the solution of this “HBT puzzle” simply requires more realistic solutions of fluid dynamics which include a full three-dimensional evolution and viscosity. Some other tantalizing features of the data, such as strong angular correlations among hadrons in the same momentum range, have not yet received a generally accepted explanation but have generated various intriguing speculations.

The many remaining questions about the nature of the matter that has been discovered at RHIC pose great challenges to experiment and theory. On the theoretical side, we need to develop tools that permit a systematic calculation of the structure of thermal QCD matter and its transport properties when the coupling is not weak. The string theory inspired techniques now used to study supersymmetric gauge theories at strong coupling promise to be useful also for real QCD. More conventional tools developed for the description of turbulent electromagnetic plasmas will perhaps allow us to solve the problem of equilibration.

On the experimental side, more measurements of rare probes which escape complete thermalization, such as heavy quarks, photons, and lepton pairs will be essential. Another important avenue for future studies are multi-particle correlations, which can give information about the medium response to a hard QCD process. Both kinds of measurements require significant detector improvements and an increase in the collider luminosity. Our capability to execute such a program will grow significantly with the RHIC luminosity upgrade and with the start of the heavy ion experiments at the Large Hadron Collider. A detailed set of measurements needed to guide theory and to discriminate between different theoretical approaches is now being planned.

6 Acknowledgements

We wish to thank Bill Zajc, Tim Hallman, Wit Busza, and Jean-Paul Blaizot for a careful reading of the manuscript and many useful suggestions. We also thank Frithjof Karsch for providing the data points in Figure 1. We acknowledge sup-

port from the United States Department of Energy grants DE-FG02-05ER41367 (Müller) and DE-FG02-00ER41152 (Nagle).

Literature Cited

1. J. W. Harris and B. Müller 1996. *Ann. Rev. Nucl. Part. Sci.* 46:71
2. A. R. Bodmer 1971. *Phys. Rev. D* 4:1601
3. T. D. Lee and G. C. Wick 1974. *Phys. Rev. D* 9:2291
4. J. C. Collins and M. J. Perry 1975. *Phys. Rev. Lett.* 34:1353
5. E. V. Shuryak 1978. *Sov. Phys. JETP* 47:212 [*Zh. Eksp. Teor. Fiz.* 74:408]
6. E. V. Shuryak 1978. *Phys. Lett. B* 78:150 [*Yad. Fiz.* 28, 796]
7. R. Hagedorn 1965. *Nuovo Cim. Suppl.* 3:147
8. M. G. Alford 2001. *Ann. Rev. Nucl. Part. Sci.* 51:131
9. R. Hagedorn and J. Rafelski 1980. *Phys. Lett. B* 97:136
10. F. Karsch 2002. *Nucl. Phys. A* 698:199
11. S. D. Katz 2005. arXiv:hep-ph/0511166.
12. F. R. Brown *et al.* 1990. *Phys. Rev. Lett.* 65:2491
13. C. Bernard *et al.* 2005. *Phys. Rev. D* 71:034504
14. O. Kaczmarek, F. Karsch, P. Petreczky and F. Zantow 2002. *Phys. Lett. B* 543:41
15. O. Kaczmarek, F. Karsch, F. Zantow and P. Petreczky 2004. *Phys. Rev. D* 70:074505 [Erratum 2005. *ibid.* D 72:059903]
16. M. Asakawa, T. Hatsuda and Y. Nakahara 2001. *Prog. Part. Nucl. Phys.* 46:459
17. E. Braaten and R. D. Pisarski 1990. *Nucl. Phys. B* 337:569
18. J. O. Andersen, E. Braaten, E. Petitgirard and M. Strickland 2002. *Phys. Rev. D* 66:085016
19. J. P. Blaizot, E. Iancu and A. Rebhan 2003. *Phys. Rev. D* 68:025011
20. E. V. Shuryak and I. Zahed 2004. *Phys. Rev. D* 70:054507
21. S. Ichimaru, 2004. *Statistical Plasma Physics* Vols. 1 and 2, (Westview, Boulder).
22. P. Kovtun, D. T. Son and A. O. Starinets 2005. *Phys. Rev. Lett.* 94:111601
23. M. Gyulassy and L. McLerran 2005. *Nucl. Phys. A* 750:30 [arXiv:nucl-th/0405013].
24. G. Baym, H. Monien, C. J. Pethick and D. G. Ravenhall 1990. *Phys. Rev. Lett.* 64:1867
25. P. Arnold, G. D. Moore and L. G. Yaffe 2000. *JHEP* 0011:001
26. G. Policastro, D. T. Son and A. O. Starinets 2001. *Phys. Rev. Lett.* 87:081601
27. V. Koch, A. Majumder and J. Randrup 2005. *Phys. Rev. Lett.* 95:182301
28. S. Ejiri, F. Karsch and K. Redlich 2005. arXiv:hep-ph/0509051.
29. G. Boyd, J. Engels, F. Karsch, E. Laermann, C. Legeland, M. Lütgemeier and B. Petersson 1996. *Nucl. Phys. B* 469:419 [arXiv:hep-lat/9602007].
30. C. M. Hung and E. V. Shuryak 1995. *Phys. Rev. Lett.* 75:4003
31. D. H. Rischke and M. Gyulassy 1996. *Nucl. Phys. A* 608:479
32. M. Asakawa, U. W. Heinz and B. Müller 2000. *Phys. Rev. Lett.* 85:2072
33. S. Jeon and V. Koch 2000. *Phys. Rev. Lett.* 85:2076
34. C. R. Allton *et al.* 2005. *Phys. Rev. D* 71:054508
35. R. V. Gavai and S. Gupta 2005. arXiv:hep-lat/0510044.
36. V. V. Klimov 1981. *Sov. J. Nucl. Phys.* 33:934 [*Yad. Fiz.* 33:1734].
37. H. A. Weldon 1982. *Phys. Rev. D* 26:2789
38. R. Rapp and J. Wambach 2000. *Adv. Nucl. Phys.* 25:1
39. K. Rajagopal and F. Wilczek 1993. *Nucl. Phys. B* 404:577 [arXiv:hep-ph/9303281].
40. For a recent review see: B. Mohanty and J. Serreau 2005. *Phys. Rept.* 414:263
41. D. Kharzeev and R. D. Pisarski 2000. *Phys. Rev. D* 61:111901
42. S. Digal, P. Petreczky and H. Satz 2001. arXiv:hep-ph/0110406.
43. M. Asakawa and T. Hatsuda 2004. *Phys. Rev. Lett.* 92:012001
44. S. Datta, F. Karsch, P. Petreczky and I. Wetzorke 2004. *Phys. Rev. D* 69:094507
45. A. Mocsy and P. Petreczky 2005. arXiv:hep-ph/0512156.
46. J. W. Qiu, J. P. Vary and X. F. Zhang 2002. *Phys. Rev. Lett.* 88:232301
47. L. Grandchamp, R. Rapp and G. E. Brown 2004. *Phys. Rev. Lett.* 92:212301
48. J. P. Blaizot and A. H. Mueller 1987. *Nucl. Phys. B* 289:847
49. A. Kovner, L. D. McLerran and H. Weigert 1995. *Phys. Rev. D* 52:6231
50. Y. V. Kovchegov 2001 *Nucl. Phys. A* 692:557
51. T. S. Biro, E. van Doorn, B. Müller, M. H. Thoma and X. N. Wang 1993. *Phys. Rev. C*

- 48:1275
52. R. Baier, A. H. Mueller, D. Schiff and D. T. Son 2001. *Phys. Lett. B* 502:51
 53. D. Molnar and M. Gyulassy 2002. *Nucl. Phys. A* 697:495 [Erratum *ibid. A* 703:893]
 54. S. M. H. Wong 1996. *Phys. Rev. C* 54:2588
 55. Z. Xu and C. Greiner 2005. *Phys. Rev. C* 71:064901
 56. S. Mrowczynski 1994. *Phys. Rev. C* 49:2191
 57. P. Arnold, J. Lenaghan, G. D. Moore and L. G. Yaffe 2005. *Phys. Rev. Lett.* 94:072302
 58. A. Rebhan, P. Romatschke and M. Strickland 2005. *JHEP* 0509:041
 59. A. Dumitru and Y. Nara 2005. *Phys. Lett. B* 621:89
 60. S. Mrowczynski 2005. arXiv:hep-ph/0511052.
 61. P. Arnold, J. Lenaghan and G. D. Moore 2003. *JHEP* 0308:002
 62. A. H. Mueller, A. I. Shoshi and S. M. H. Wong 2006. *Phys. Lett. B* 632:257
 63. F. Karsch, E. Laermann, P. Petreczky, S. Stickan and I. Wetzorke 2002. *Phys. Lett. B* 530:147
 64. P. Petreczky 2004. *J. Phys. G* 30:S431
 65. J. P. Blaizot and F. Gelis 2005. *Eur. Phys. J. C* 43:375
 66. P. Petreczky, K. Petrov, D. Teaney and A. Velytsky 2005. *Proceed. Lattice 2005*:185
 67. J. M. Maldacena 1998. *Adv. Theor. Math. Phys.* 2:231 [1999. *Int. J. Theor. Phys.* 38:1113]
 68. de Teramond G.F., Brodsky S.J. 2005. *Phys. Rev. Lett.* 94:201601. Polchinski J, Strassler M.J. 2002. *Phys. Rev. Lett.* 88:031601. Brower R.C. 2005. *Acta Phys. Polon. B* 34:5927.
 69. H. Satz and X. N. Wang 1995. *Int. J. Mod. Phys. A* 10:2881
 70. A. Accardi *et al.* 2003. arXiv:hep-ph/0310274.
 71. A. Accardi *et al.*, 2003. arXiv:hep-ph/0308248.
 72. P. R. Norton 2003. *Rept. Prog. Phys.* 66:1253
 73. L. V. Gribov, E. M. Levin and M. G. Ryskin 1983. *Phys. Rept.* 100:1
 74. L. McLerran 2002. *Nucl. Phys. A* 702:49
 75. A. H. Mueller and J. W. Qiu 1986. *Nucl. Phys. B* 268:427
 76. L. D. McLerran and R. Venugopalan 1994. *Phys. Rev. D* 49:2233
 77. D. Kharzeev, E. Levin and L. McLerran 2003. *Phys. Lett. B* 561:93
 78. R. Baier, Y. L. Dokshitzer, A. H. Mueller, S. Peigne and D. Schiff 1997. *Nucl. Phys. B* 483:291
 79. R. Baier, D. Schiff and B. G. Zakharov 2000. *Ann. Rev. Nucl. Part. Sci.* 50:37
 80. L. D. Landau and I. Pomeranchuk 1953. *Dokl. Akad. Nauk Ser. Fiz.* 92:535
 81. A. B. Migdal 1956. *Phys. Rev.* 103:1811
 82. R. Baier, Y. L. Dokshitzer, A. H. Mueller and D. Schiff 2001. *JHEP* 0109:033
 83. C. A. Salgado and U. A. Wiedemann 2003. *Phys. Rev. D* 68:014008
 84. E. V. Shuryak 2002. *Phys. Rev. C* 66:027902
 85. B. Müller 2003. *Phys. Rev. C* 67:061901
 86. K. J. Eskola, H. Honkanen, C. A. Salgado and U. A. Wiedemann 2005. *Nucl. Phys. A* 747:511
 87. M. Bedjidian *et al.* 2003. arXiv:hep-ph/0311048.
 88. Y. L. Dokshitzer and D. E. Kharzeev 2001. *Phys. Lett. B* 519:199
 89. Y. L. Dokshitzer, V. A. Khoze and S. I. Troian 1991. *J. Phys. G* 17:1602
 90. S. Hannestad 2004. *Phys. Rev. D* 70:043506
 91. T. DeGrand and K. Kajantie 1984. *Phys. Lett. B* 147:273
 92. D. J. Schwarz 2003. *Annalen Phys.* 12:220
 93. E. Witten 1984. *Phys. Rev. D* 30:272
 94. D. J. Schwarz 1998. *Mod. Phys. Lett. A* 13:2771
 95. M. H. Thoma 2005. arXiv:hep-ph/0509154.
 96. M. H. Thoma 2005. *J. Phys. G* 31:L7
 97. O'Hara K.M. *et al.* 2002. *Science* 298:2179 Bourdel T. *et al.* 2003. *Phys. Rev. Lett.* 91:020402.
 98. Harrison M, Peggs S., Roser T. 2002. *Ann. Rev. Nucl. Part. Sci.* 52:425.
 99. Addamczyk M. *et al.* 2003. *Nucl. Instrum. Meth. A* 499:437. Adcox K. *et al.* 2003. *Nucl. Instrum. Meth. A* 499:469. Back B.B. *et al.* 2003. *Nucl. Instrum. Meth. A* 499:603. Ackermann K.H. *et al.* 2003. *Nucl. Instrum. Meth. A* 499:624.
 100. Arsene I. *et al.* 2005. *Nucl. Phys. A* 757:1.
 101. Adcox K. *et al.* 2005. *Nucl. Phys. A* 757:184.
 102. Back B.B. *et al.* 2005. *Nucl. Phys. A* 757:28.

103. Adams J. *et al.* 2005. *Nucl. Phys. A* 757:102.
104. Bearden I.G. *et al.* 2004. *Phys. Rev. Lett.* 93:102301.
105. Back B.B. *et al.* 2003. *Phys. Rev. Lett.* 91:052303.
106. Li S.-y., Wang, X.-N. 2002. *Phys. Lett. B* 527, 85.
107. Kharzeev D., Nardi M. 2001. *Phys. Lett. B* 507, 121. Kharzeev D., Levin E., 2001. *Phys. Lett. B* 523, 79.
108. Mueller A.H. 1983. *Nucl. Phys. B* 213, 85.
109. Bjorken J.D. 1983. *Phys. Rev. D* 27:140-151.
110. T. Hirano and Y. Nara 2004 *Phys. Rev. C* 69:034908
111. Kaneta M., Xu, N. 2004. nucl-th/0405068.
112. Braun-Munzinger P., Magestro D., Redlich K., Stachel J. 2001. *Phys. Lett. B* 518, 41.
113. Becattini F., Heinz U.W. 1997. *Z Phys. C* 76, 269 (e).
114. Adams J. *et al.* 2005. *Phys. Rev. C* 71, 064902.
115. Bearden I.G. *et al.* 2005. *Phys. Rev. Lett.* 94:162301.
116. Fermi E. 1950. *Prog. Theor. Phys.* 5, 570. Landau L.D. 1953. *Izv. Akad. Nauk Ser. Fiz.* 17, 51. Landau L.D., Belenkij S.Z. 1956. *Nuovo Cim. Suppl.* 3S10, 15. Carruthers P, Doughton, 1973. *Phys. Rev. D* 8, 859. Steinberg P. 2005. *Acta Phys. Hung.* A24:51-57.
117. Bearden I.G. *et al.* 2003. *Phys. Rev. Lett.* 90:102301.
118. Kharzeev D., Pisarski R.D. *Phys. Rev. D* 61:111901.
119. Adams J. *et al.* 2005. *Phys. Rev. C* 72, 044902. Adams J. *et al.* 2005. *Phys. Rev. C* 71, 064906.
120. Bass S.A., Danielewicz P., Pratt S. 2000. *Phys. Rev. Lett.* 85, 2689.
121. Kolb P.F., Sollfrank J., Heinz U.W. 2000. *Phys. Rev. C* 62, 054909.
122. Ollitrault J.Y. 1992. *Phys. Rev. D* 46:229-245. Poskanzer A.M., Voloshin S.A. 1998. *Phys. Rev. C* 58, 1671. Borghini N., Dinh, P.M., Ollitrault, J.Y. 2001. *Phys. Rev. C* 64, 054901.
123. Hanbury-Brown R. and Twiss R. 1954. *Phil. Mag.* 45, 663.
124. Wiedemann U. and Heinz U. 1999. *Phys. Rep.* 319, 145.
125. Adams J. *et al.* 2005. *Phys. Rev. C* 71:044906.
126. Back B.B. *et al.* 2005. *Phys. Rev. C* 72:051901. Back B.B. *et al.* 2005. *Phys. Rev. Lett.* 94:122303.
127. Bhalerao R.S., Blaizot J.P., Borghini N., Ollitrault J.Y. 2005. *Phys. Lett. B* 627, 49.
128. Adams J. *et al.* 2005. *Phys. Rev. Lett.* 95:122301.
129. Okubo S. 1977. *Phys. Rev. D* 16:2336.
130. Egusa T. 1979. *Prog. Theor. Phys.* 61:356.
131. Adams J. *et al.* 2005. *Phys. Rev. C* 72, 014904.
132. Wang F. *et al.* 2005. nucl-ex/0510068
133. van Hecke H. *et al.* 1998. *Phys. Rev. Lett.* 81:5764.
134. Cassing W., Gallmeister K., Greiner C. 2004. *Nucl. Phys. A* 735:277. Bratkovskaya E.L., Cassing W., Stocker H. 2003. *Phys. Rev. C* 67:054905. Bleicher M, Stocker H. 2002. Anisotropic Flow in Ultrarelativistic Heavy Ion Collisions. *Phys. Lett. B* 26:309.
135. Greiner C. 2003. *Nucl. Phys. A* 715, 75.
136. Abreu P. *et al.* 2000. *Eur. Phys. J C* 17, 207.
137. Adler S.S. *et al.* 2004. *Phys. Rev. C* 69:034909.
138. C. Adler *et al.*, *Phys. Rev. Lett.* 89:092301 (2002). J. Adams *et al.* [STAR Collaboration], *Phys. Rev. Lett.* 92:052302 (2004).
139. Sorensen P.R. 2005. arXiv:nucl-ex/050052.
140. Adler S.S. *et al.* 2005. *Phys. Rev. C* 72, 014903. Adams J. *et al.* 2005. *Phys. Rev. B* 612, 181.
141. R. J. Fries, B. Müller, C. Nonaka and S. A. Bass 2003. *Phys. Rev. Lett.* 90:202303
142. Adler S.S. *et al.* 2005. *Phys. Rev. C* 71:051902(R).
143. Batsouli S. *et al.* 2003. *Phys. Lett. B* 557, 26.
144. Adler S.S. *et al.* 2005. *Phys. Rev. C* 72:024901. Nagle J.L. *et al.* 2005. nucl-ex/0509024.
145. Adams J. *et al.* 2003. *Phys. Rev. Lett.* 91:072304. Arsene I. *et al.* 2003. *Phys. Rev. Lett.* 91:072305. Adler S.S. *et al.* 2003. *Phys. Rev. Lett.* 91:072303. Back B.B. *et al.* 2003. *Phys. Rev. Lett.* 91:072302.
146. Antreasyan *et al.* 1979. *Phys. Rev. D* 19, 764.
147. Adler S.S. *et al.* 2005. *Phys. Rev. Lett.* 94:082302. Arsene I. *et al.* 2004. *Phys. Rev. Lett.* 93:232303. Back B.B. *et al.* 2004. *Phys. Rev. C* 70:061901.
148. Adler S.S. *et al.* 2005. *Phys. Rev. Lett.* 94:232301. Adler S.S. *et al.* 2005. *Phys. Rev. D*

- 71:071102.
149. Reygers K. *et al.* 2005. arXiv:hep-ex/0512015
 150. Adams J. *et al.* 2005. *Phys. Rev. Lett.* 94:062301.
 151. Adler S.S. *et al.* 2005. nucl-ex/0510047 Dunlop J.C. *et al.* 2005. nucl-ex/0510073.
 152. Adams J. *et al.* 2003. *Phys. Rev. Lett.* 90:082302.
 153. Adams J. *et al.* 2005. *Phys. Rev. Lett.* 95:152301. Adler S.S. *et al.* 2005. arXiv:nucl-ex/0507004
 154. Busching H. *et al.* 2005. arXiv:nucl-ex/0511044.
 155. Matsui T., Satz H. 1986. *Phys. Lett. B* 178, 416.
 156. Adler S.S. *et al.* 2006. *Phys. Rev. Lett.* 91, 012304.
 157. Pereira Da Costa H. *et al.* 2005. arXiv:nucl-ex/0510051.
 158. Abreu M.C. *et al.* 2001. *Phys. Lett. B* 521:195.
 159. Rapp R. 2005. *Eur. Phys. J.C* 43, 91. Thews R.L. 2005. *Eur. Phys. J.C* 43, 97.
 160. P. Huovinen, P. F. Kolb and U. W. Heinz 2002. *Nucl. Phys. A* 698:475
 161. P. F. Kolb, U. W. Heinz, P. Huovinen, K. J. Eskola and K. Tuominen 2001. *Nucl. Phys. A* 696:197
 162. F. Retiere and M. A. Lisa 2004. *Phys. Rev. C* 70:044907
 163. P. F. Kolb, J. Sollfrank and U. W. Heinz 2000. *Phys. Rev. C* 62:054909
 164. U. W. Heinz and P. F. Kolb 2002. *Nucl. Phys. A* 702:269
 165. D. Teaney, J. Lauret and E. V. Shuryak 2001. arXiv:nucl-th/0110037.
 166. P. Huovinen 2005 *Nucl. Phys. A* 761:296
 167. D. Teaney 2003. *Phys. Rev. C* 68:034913
 168. T. Hirano and M. Gyulassy 2005. arXiv:nucl-th/0506049.
 169. T. Hirano and Y. Nara 2004. *Nucl. Phys. A* 743:305
 170. C. Nonaka and S. A. Bass 2005. arXiv:nucl-th/0510038.
 171. Z. w. Lin and D. Molnar 2003. *Phys. Rev. C* 68:044901
 172. V. Greco, C. M. Ko and R. Rapp 2004. *Phys. Lett. B* 595:202
 173. E. Braaten, Y. Jia and T. Mehen 2002. *Phys. Rev. D* 66:014003
 174. R. Baier 2003. *Nucl. Phys. A* 715:209
 175. I. Vitev and M. Gyulassy 2002. *Phys. Rev. Lett.* 89:252301
 176. I. Vitev 2004. *J. Phys. G* 30:S791
 177. S. Pal and S. Pratt 2004. *Phys. Lett. B* 578:310
 178. M. Djordjevic, M. Gyulassy, R. Vogt and S. Wicks 2006. *Phys. Lett. B* 632:81
 179. M. G. Mustafa 2005. *Phys. Rev. C* 72:014905
 180. G. D. Moore and D. Teaney 2005. *Phys. Rev. C* 71:064904
 181. H. van Hees and R. Rapp 2005. *Phys. Rev. C* 71:034907
 182. S. Wicks, W. Horowitz, M. Djordjevic and M. Gyulassy 2005. arXiv:nucl-th/0512076.
 183. C. Nonaka, B. Muller, S. A. Bass and M. Asakawa 2005. *Phys. Rev. C* 71:051901
 184. B. Müller and K. Rajagopal 2005. *Eur. Phys. J. C* 43:15
 185. V. Greco, C. M. Ko and P. Levai 2003. *Phys. Rev. Lett.* 90:202302
 186. V. Greco, C. M. Ko and P. Levai 2003. *Phys. Rev. C* 68:034904
 187. R. J. Fries, B. Müller, C. Nonaka and S. A. Bass 2003. *Phys. Rev. C* 68:044902
 188. J. Rafelski and B. Müller 1982. *Phys. Rev. Lett.* 48:1066 [Erratum 1986. *ibid.* 56:2334]
 189. B. Müller, R. J. Fries and S. A. Bass 2005. *Phys. Lett. B* 618:77
 190. A. Majumder and B. Müller, 2006. in preparation
 191. Sorge H. 1994. *Phys. Rev. C* 49, 1253.
 192. Back B.B. *et al.* 2001. *Phys. Rev. Lett* 87, 242301. Armstrong T.A. *et al.* 1999. *Phys. Rev. C* 59, 2699.
 193. U. W. Heinz and M. Jacob, arXiv:nucl-th/0002042.
 194. U. W. Heinz, private communication.
 195. Abreu M.C. *et al.* 2000. *Phys. Lett. B* 477, 28.
 196. Cole B.A. *et al.* 2005. nucl-ex/0503009 Chemakin I. *et al.* 2000. *Phys. Rev. Lett.* 85, 4868.
 197. T. Susa 2002. *Nucl. Phys. A* 698:491
 198. Arnaldi R. *et al.* 2005. *Eur. Phys. J.C* 43, 167. Shahoian R. *et al.* 2005. *Eur. Phys. J.C* 43, 209. Usai G.C. *et al.* 2005. *Eur. Phys. J.C* 43, 415.
 199. Hohne C. *et al.* 2005. arXiv:nucl-ex/0510049
 200. Agakichiev G. *et al.* 2005. *Eur. Phys. J.C* 41, 475. Bielcikova J. *et al.* 2005. *Eur. Phys. J.C* 43, 323.
 201. Senger P. 2004. *J. Phys. G* 30, S1087.

- Damjonovic S. *et al.* 2005. nucl-ex/0510044.
202. Agakishiev G. *et al.* 1998. *Phys. Lett. B* 422, 405.
203. Debasish D. *et al.* 2005. nucl-ex/0511055
204. Mangano M.L., Satz H., Wiedermann U.A. (eds) 2004. (CERN Yellow Report) CERN-2004-009, ISBN 92-9083-234-7.
205. L. McLerran 2005. *Nucl. Phys. A* 752:355
206. A. Krasnitz, Y. Nara and R. Venugopalan 2003. *Nucl. Phys. A* 717:268
207. A. Krasnitz, Y. Nara and R. Venugopalan 2003. *Nucl. Phys. A* 727:427
208. T. Lappi 2003. *Phys. Rev. C* 67:054903
209. B. Müller and A. Schäfer 2005. arXiv:hep-ph/0512100.
210. B. Müller and A. Schäfer 2003. arXiv:hep-ph/0306309.
211. E. V. Shuryak and I. Zahed 2003. *Phys. Rev. D* 67:054025
212. I. R. Klebanov 2005. arXiv:hep-ph/0509087.
213. S. Catterall 2005. arXiv:hep-lat/0510054.
214. P. Hartmann, Z. Donko, P. Levai and G. J. Kalman 2006. arXiv:nucl-th/0601017.
215. B. A. Gelman, E. V. Shuryak and I. Zahed 2006. arXiv:nucl-th/0601029.
216. T. Hirano and K. Tsuda 2002. *Phys. Rev. C* 66:054905
217. Y. Hama, R. P. G. Andrade, F. Grassi, O. J. Socolowski, T. Kodama, B. Tavares and S. S. Padula 2005. arXiv:hep-ph/0510096.
218. J. Ruppert and B. Müller 2005. *Phys. Lett. B* 618:123
219. J. Casalderrey-Solana, E. V. Shuryak and D. Teaney 2004. arXiv:hep-ph/0411315.
220. L. M. Satarov, H. Stöcker and I. N. Mishustin 2005. *Phys. Lett. B* 627:64
221. I. M. Dremin 2005. arXiv:hep-ph/0507167.
222. V. Koch, A. Majumder and X. N. Wang 2005. arXiv:nucl-th/0507063.
223. T. Renk and J. Ruppert 2005. arXiv:hep-ph/0509036.
224. J. A. Lopez, J. C. Parikh and P. J. Siemens 1984. *Phys. Rev. Lett.* 53:1216
225. C. Adler *et al.* 2003. *Phys. Rev. Lett.* 90:082302
226. S. S. Adler *et al.* 2005. *Phys. Rev. C* 71:051902
227. R. C. Hwa and C. B. Yang 2004. *Phys. Rev. C* 70:024905
228. R. J. Fries, S. A. Bass and B. Müller 2005. *Phys. Rev. Lett.* 94:122301
229. A. Majumder, E. Wang and X. N. Wang 2005. arXiv:nucl-th/0506040.

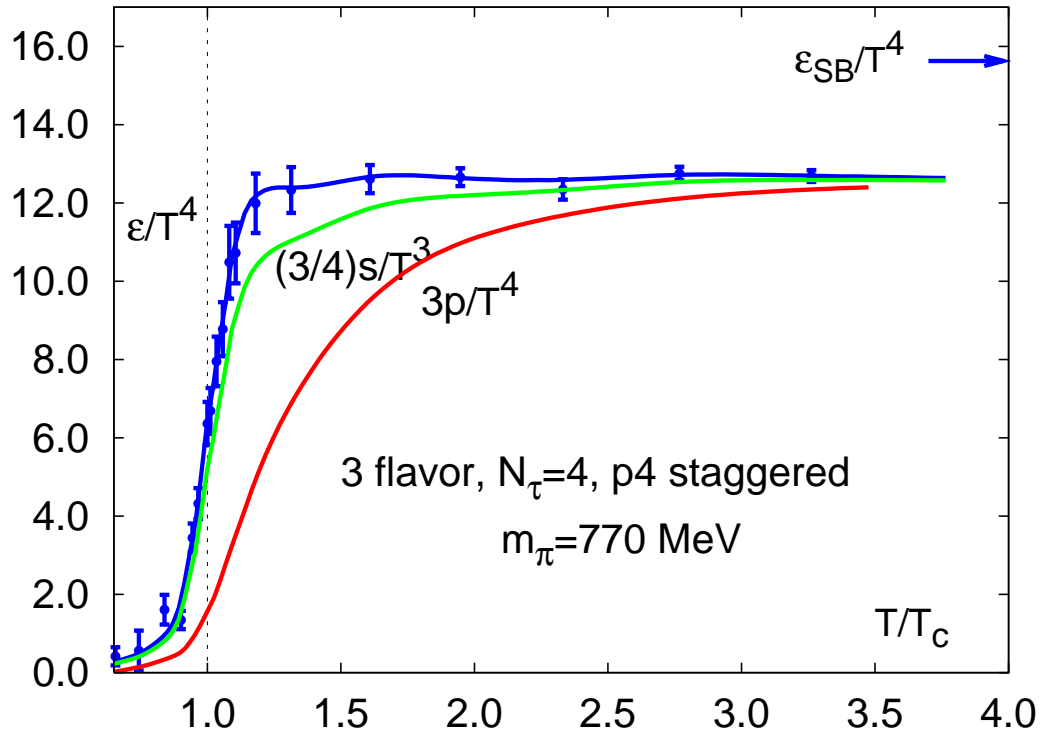


Figure 1: Figure of $\varepsilon(T)/T^4$, $P(T)/T^4$, and $s(T)/T^3$ for three light flavors of quarks on the lattice.

Table 1: Table of RHIC Performance.

Run	Species	Particle Energy [GeV/n]	Total Delivered Luminosity	Average Store Polarization
Run-1 2000	<i>Au + Au</i>	27.9	$< 0.001 \mu b^{-1}$	-
	<i>Au + Au</i>	65.2	$20 \mu b^{-1}$	-
Run-2 2001-2	<i>Au + Au</i>	100.0	$258 \mu b^{-1}$	-
	<i>Au + Au</i>	9.8	$0.4 \mu b^{-1}$	-
Run-3 2002-3	pol. <i>p + p</i>	100.0	$1.4 \mu b^{-1}$	14%
	<i>d + Au</i>	100.0	$1.4 pb^{-1}$	-
	pol. <i>p + p</i>	100.0	$5.5 pb^{-1}$	34%
Run-4 2003-4	<i>Au + Au</i>	100.0	$3740 \mu b^{-1}$	-
	<i>Au + Au</i>	31.2	$67 \mu b^{-1}$	-
	pol. <i>p + p</i>	100.0	$7.1 pb^{-1}$	45%
Run-5 2004-5	<i>Cu + Cu</i>	100.0	$42.1 nb^{-1}$	-
	<i>Cu + Cu</i>	31.2	$67 \mu b^{-1}$	-
	<i>Cu + Cu</i>	11.2	$0.02 nb^{-1}$	-
	pol. <i>p + p</i>	100.0	$29.5 pb^{-1}$	46%
	pol. <i>p + p</i>	204.9	$0.1 pb^{-1}$	30%

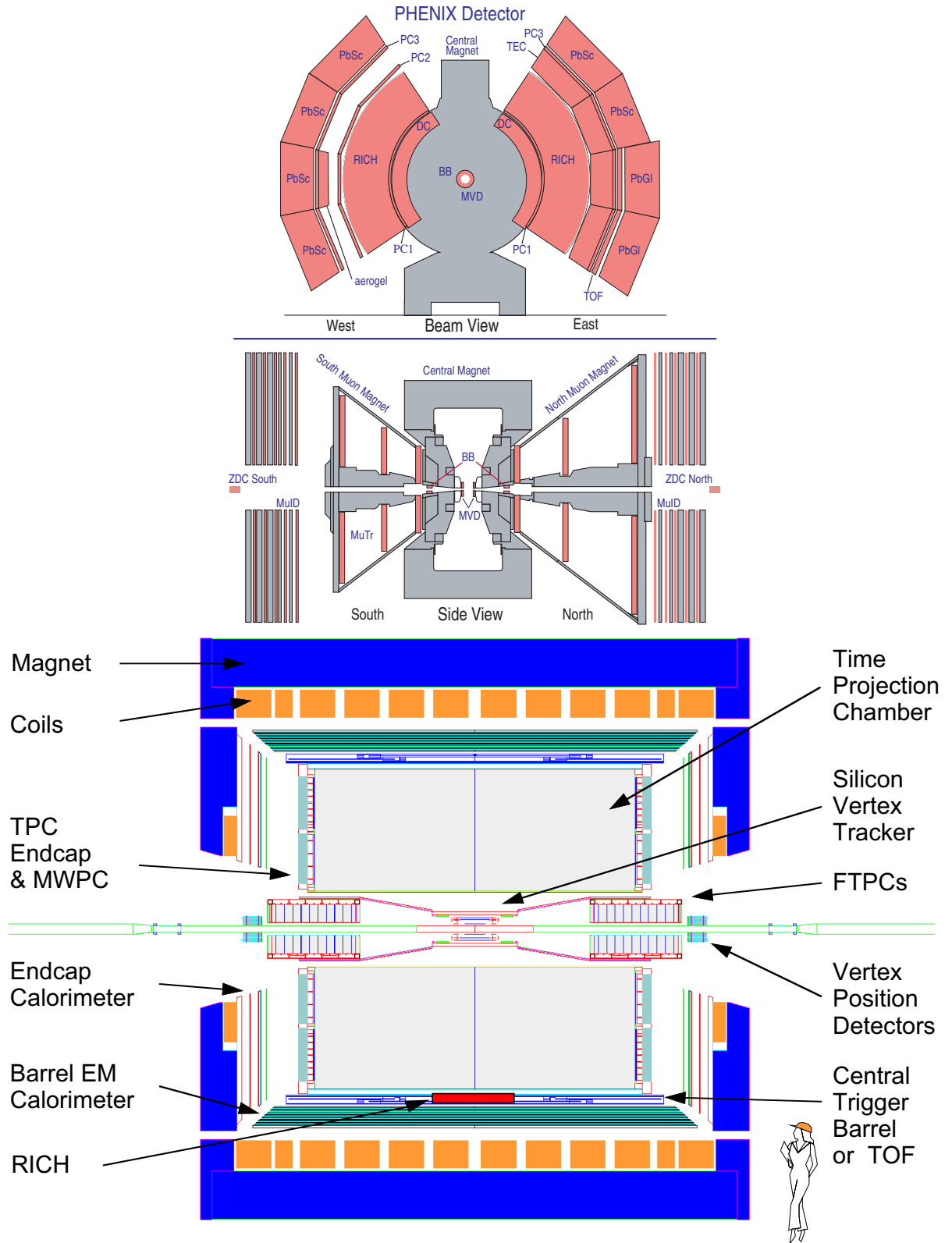


Figure 2: Schematic diagrams of the PHENIX (above) and STAR (below) experiment configurations. Details of the various detector subsystems are given in (99)

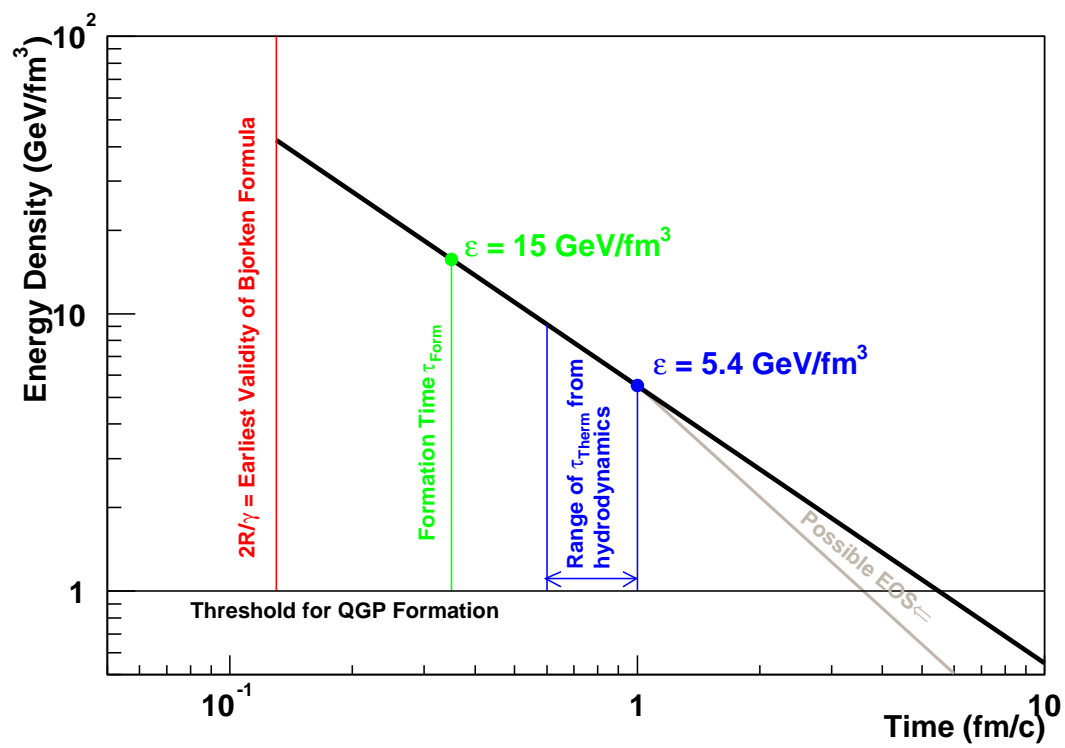


Figure 3: Schematic drawing of the time and energy density scales derived through the Bjorken picture. Taken from (101).

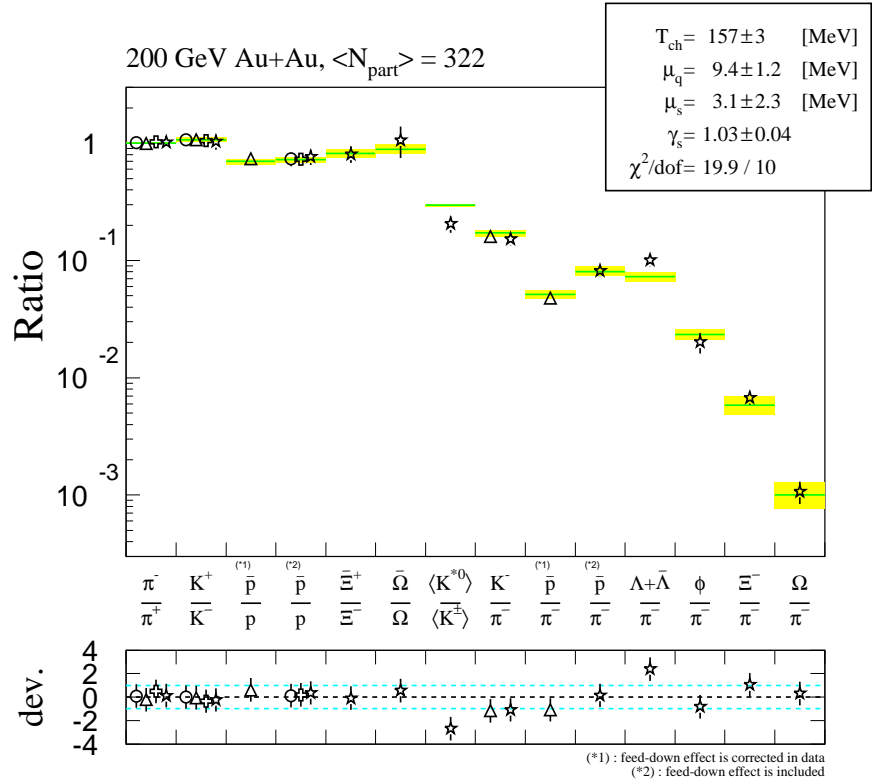


Figure 4: Comparison of BRAHMS (circles), PHENIX (triangles), PHOBOS (crosses) and STAR (stars) particle ratios from central gold-gold collisions at $\sqrt{s_{NN}} = 200$ GeV at mid-rapidity. The thermal model descriptions from (111) are also shown as lines. Similar results are obtained in (112).

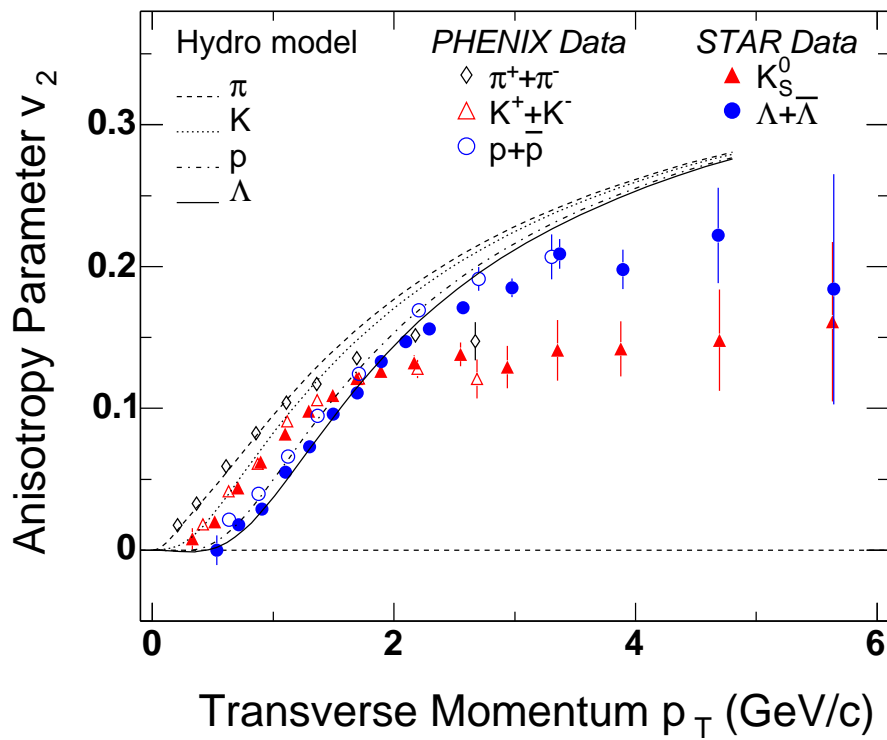


Figure 5: Azimuthal anisotropy (v_2) as a function of p_T from minimum bias gold-gold collisions (101, 131). Hydrodynamic calculations are shown as dashed lines.

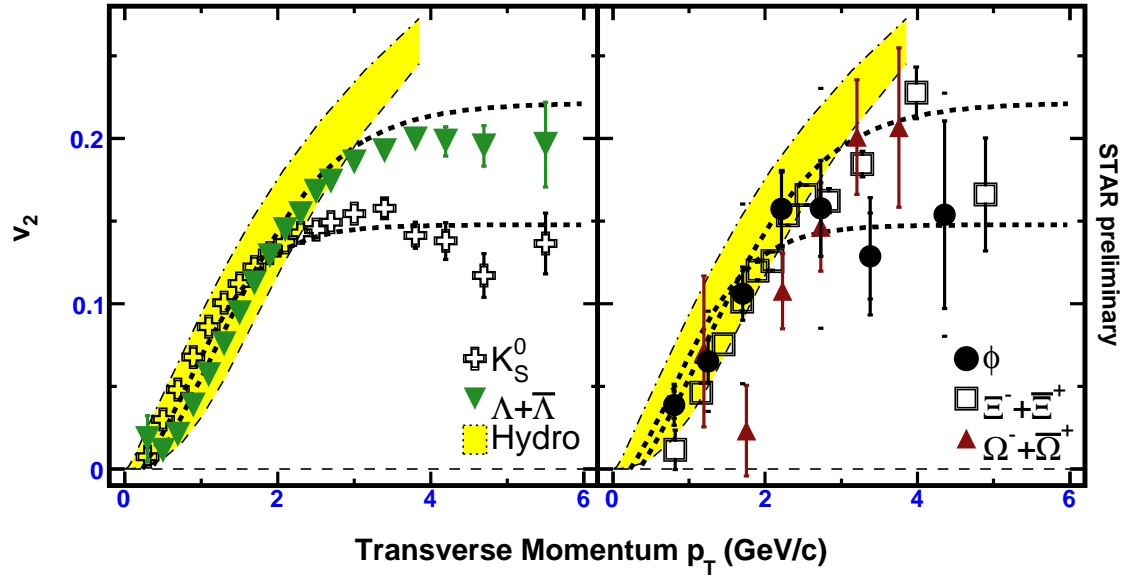


Figure 6: Azimuthal anisotropy (v_2) for strange (left) and multi-strange (right) hadrons from the STAR experiment (132). The curves are empirical fits. The shaded areas are ranges of hydrodynamic calculation results.

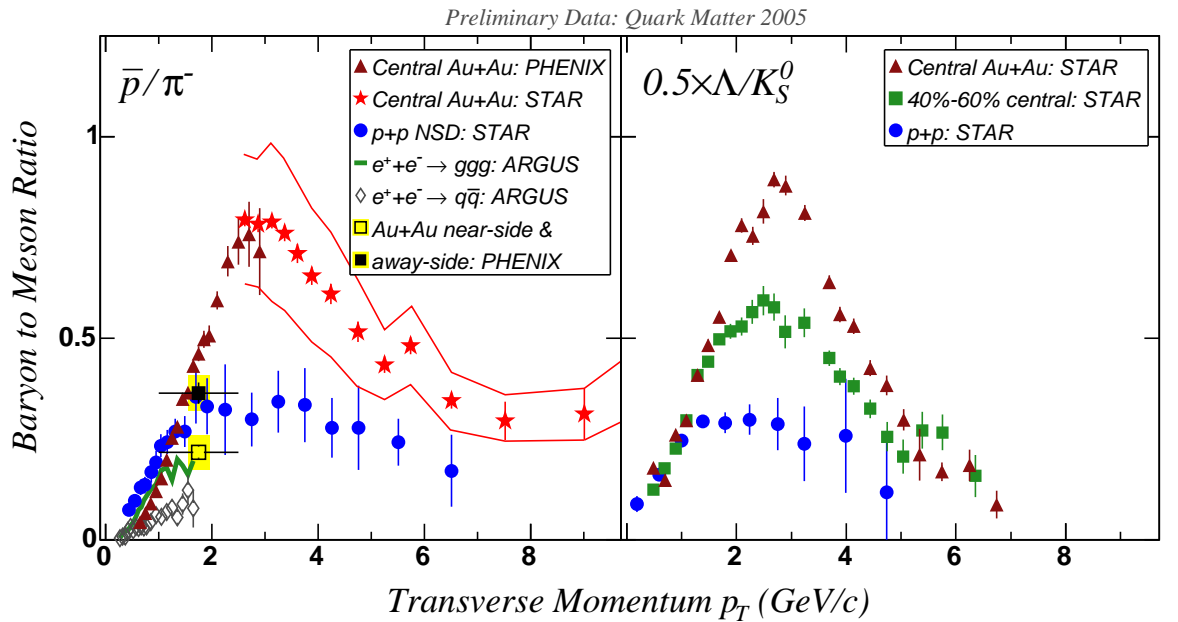


Figure 7: (Left) The \bar{p}/π^- ratio at mid-rapidity for central gold-gold and proton-proton collisions. (Right) The Λ/K_S^0 ratio in central and mid-central gold-gold collisions and minimum bias proton-proton collisions. Values as scaled by 0.5.

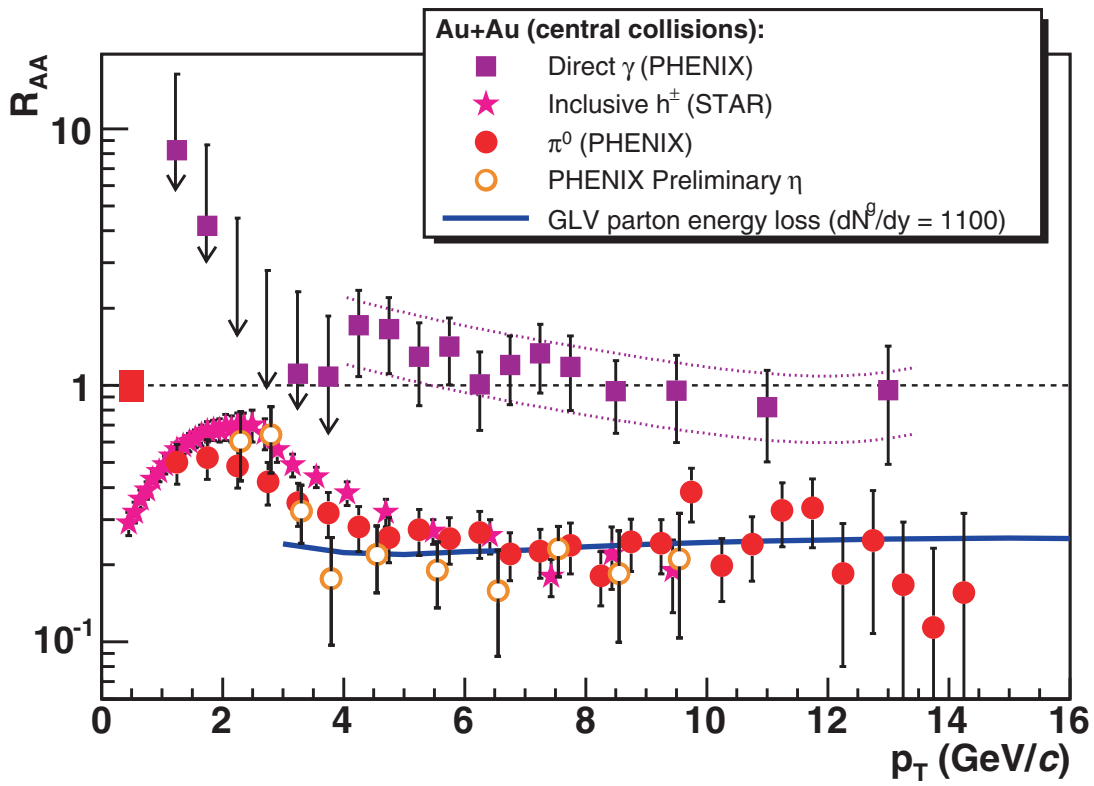


Figure 8: Nuclear modification factor R_{AA} for direct photons and hadrons in central (0-10% of σ_{inel}^{Au+Au}) gold-gold collisions at $\sqrt{s_{NN}} = 200$ GeV (149).

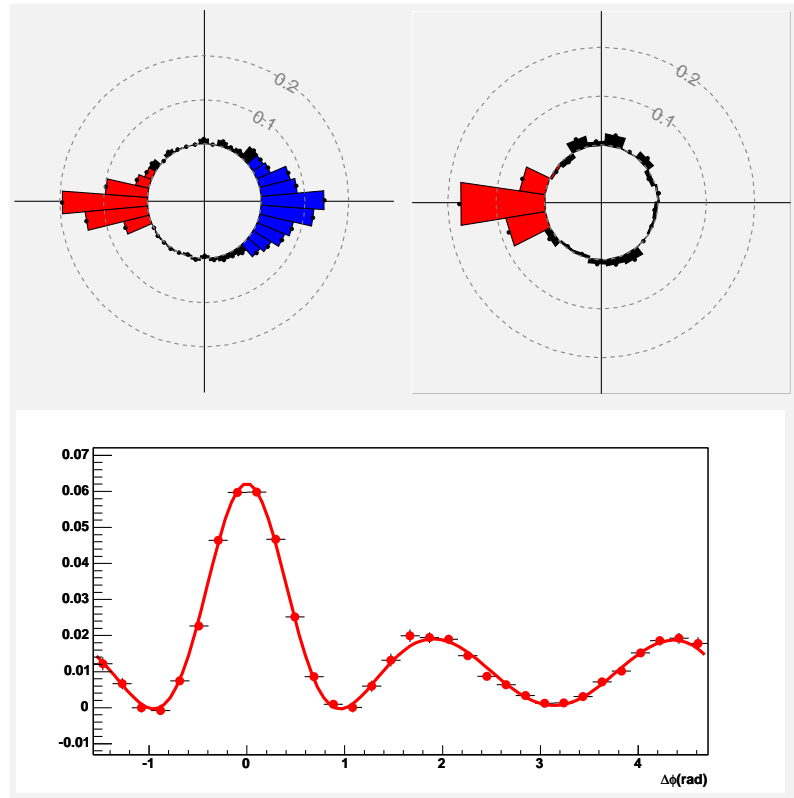


Figure 9: Upper panels results from the STAR experiment are the azimuthal distributions of unidentified hadron pairs for (left) proton-proton reactions and (right) background subtracted central gold-gold reactions. All correlation functions require a trigger particle with $4 < p_T < 6$ GeV/c and associated particles with $p_T > 2$ GeV/c. The lower panel are preliminary results from the PHENIX experiment on the azimuthal distribution in central gold-gold reactions requiring the trigger particle $2.5 < p_T < 4.0$ GeV/c and the associated particles with $2.0 < p_T < 3.0$ GeV/c.

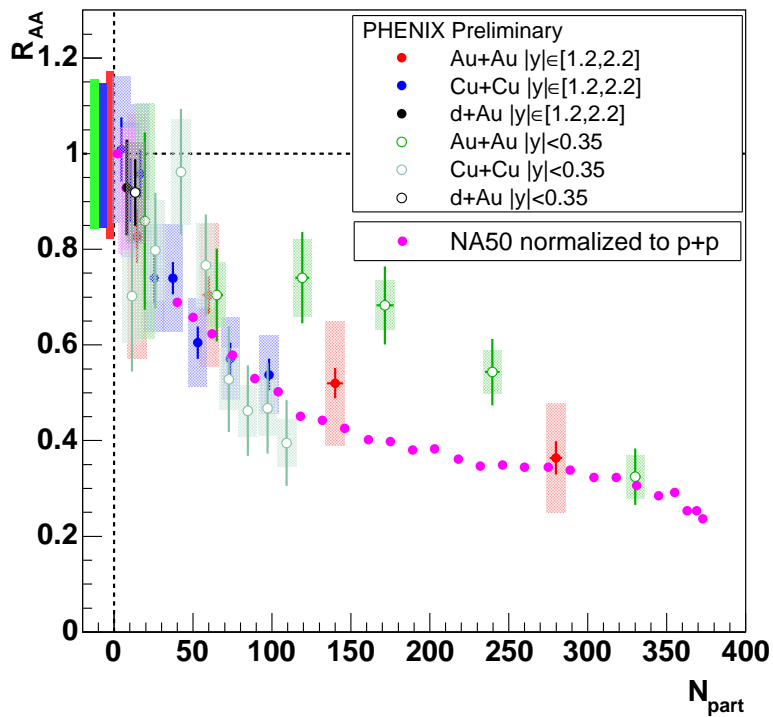


Figure 10: PHENIX preliminary results on J/ψ nuclear modification factor R_{AA} as a function of the number of nuclear participants (157). Results are shown from gold-gold, copper-copper, and deuteron-gold reactions at forward and mid-rapidity. Also shown are results from the NA50 experiment from lower energy at the CERN-SPS (158).